

Enhanced Sparsity by Non-Separable Regularization

Ivan Selesnick and İlker Bayram

Abstract

This paper develops a convex approach for sparse one-dimensional deconvolution that improves upon L1-norm regularization, the standard convex approach. We propose a sparsity-inducing non-separable non-convex bivariate penalty function for this purpose. It is designed to enable the convex formulation of ill-conditioned linear inverse problems with quadratic data fidelity terms. The new penalty overcomes limitations of separable regularization. We show how the penalty parameters should be set to ensure that the objective function is convex, and provide an explicit condition to verify the optimality of a prospective solution. We present an algorithm (an instance of forward-backward splitting) for sparse deconvolution using the new penalty.

1 Introduction

Methods for sparse regularization can be broadly categorized as convex or non-convex. In the standard convex approach, the regularization terms (penalty functions) are convex; and the objective function, consisting of both data fidelity and regularization terms, is convex [4, 61]. The convex approach has several benefits: the objective function is free of extraneous local minima, and globally convergent optimization algorithms can be leveraged [11].

Despite the attractive properties of convex regularization, non-convex regularization often performs better [12, 14, 58]. Classical and recent examples are in edge preserving tomography [15, 39, 57, 59] and compressed sensing [16, 19, 76], respectively. In the non-convex approach, penalty functions are non-convex as they can be designed to induce sparsity more effectively than convex ones. However, the convexity of the objective function is generally sacrificed. Consequently, non-convex regularization is hampered by complications: the objective function will generally possess many sub-optimal local minima in which optimization algorithms can become entrapped.

It turns out, non-convex penalties can be utilized without giving up the convexity of the objective function and corresponding benefits. This is achieved by carefully specifying the penalty in accordance with the data fidelity term, as described by Blake, Zimmerman, and Nikolova [9, 56, 57, 59]. In recent work, a class of sparsity-inducing non-convex penalties has been developed to formulate convex objective functions and applied to several signal estimation problems [6, 7, 21, 29, 47, 62, 63, 70, 71]. This approach maintains the benefits of the convex framework (absence of spurious local minima, etc.), yet estimates sparse signals more accurately than convex regularization (e.g., the ℓ_1 norm) due to the sparsity-inducing properties of non-convex regularization. However, this previous work considers only *separable* (additive) penalties, which have fundamental limitations.

I. Selesnick, Electrical and Computer Engineering Dept, Tandon School of Engineering, New York University, NY, USA.

İ Bayram, Electronics and Communication Engineering Dept, Istanbul Technical University, Istanbul, Turkey.

Email: selesi@nyu.edu, ilker.bayram@itu.edu.tr

This research was supported by NSF under grant CCF-1525398.

Last Edit: September 21, 2018 5:55pm.

In this paper, we introduce a parameterized sparsity-inducing non-separable non-convex bivariate penalty function. The penalty is designed to enable the convex formulation of ill-conditioned linear inverse problems with quadratic data fidelity terms. The new penalty overcomes limitations of separable non-convex regularization. We show how the penalty parameters should be set to ensure the objective function is convex. We also show how this bivariate penalty can be incorporated into linear inverse problems of N variables ($N > 2$), and we provide an explicit condition to verify the optimality of a prospective solution. We derive two iterative algorithms for optimization using the new penalty, and demonstrate its effectiveness for one-dimensional sparse deconvolution.

1.1 Basic problem statement

We consider the problem of bivariate sparse regularization (BISR) with a quadratic data fidelity term:

$$\hat{x} = \arg \min_{x \in \mathbb{R}^2} \left\{ f(x) = \frac{1}{2} \|y - Hx\|_2^2 + \lambda \psi(x) \right\} \quad (1)$$

where $\lambda > 0$, H is a 2×2 matrix, and $\psi: \mathbb{R}^2 \rightarrow \mathbb{R}$ is a bivariate penalty. [In Sec. 5, it will be shown how to extend this bivariate problem to an N -point linear inverse problem.] In this paper, we suppose $H^\top H$ is Toeplitz, as this naturally arises in deconvolution problems. Correspondingly, we write $H^\top H = K(\gamma)$ where $\gamma = (\gamma_1, \gamma_2) \in \mathbb{R}^2$ and

$$K(\gamma) := \frac{1}{2} \begin{bmatrix} \gamma_1 + \gamma_2 & \gamma_1 - \gamma_2 \\ \gamma_1 - \gamma_2 & \gamma_1 + \gamma_2 \end{bmatrix} = Q \Gamma Q^\top \quad (2)$$

where

$$Q = \frac{1}{\sqrt{2}} \begin{bmatrix} 1 & 1 \\ 1 & -1 \end{bmatrix}, \quad \Gamma = \begin{bmatrix} \gamma_1 & 0 \\ 0 & \gamma_2 \end{bmatrix}. \quad (3)$$

This is an eigenvalue decomposition of $H^\top H$. The parameters γ_1 and γ_2 are the eigenvalues of the positive semidefinite matrix $H^\top H$; hence, they are nonnegative.

First, suppose ψ is a separable convex penalty, e.g., $\psi(x) = |x_1| + |x_2|$ corresponding to the ℓ_1 norm (Fig. 1(a)). Then the objective function f in (1) is convex, but it does not induce sparsity as effectively as non-convex penalties can. In particular, ℓ_1 norm regularization tends to underestimate the true signal values.

Second, suppose ψ is a separable non-convex penalty, i.e., $\psi(x) = \phi(x_1) + \phi(x_2)$, as illustrated in Fig. 1(b). Then the objective function f is convex only if ϕ is suitably chosen. In particular, for the class of penalties we consider, the objective function is convex only if $\phi''(t) \geq -\min\{\gamma_1, \gamma_2\}/\lambda$, where γ_1 and γ_2 are the eigenvalues of $H^\top H$. (See Lemma 3, [70], and [9].) When H is singular, the minimum eigenvalue of $H^\top H$ is zero and ϕ must be convex (i.e., it induces sparsity relatively weakly). Hence, if H is singular and we restrict the penalty ψ to be separable, then we can not use sparsity-inducing non-convex regularization without sacrificing the convexity of the objective function f . Indeed, when separable non-convex penalties are utilized for their strong sparsity-inducing properties, the convexity of f is generally sacrificed.

Our aim is to prescribe a non-separable penalty ψ so that the objective function is guaranteed to be convex even though the penalty ψ itself is not. Such a penalty will be given in Sec. 4. It turns out, when we utilize a *non-separable* non-convex penalty to strongly induce sparsity, we need *not* sacrifice the convexity of the objective function f , even when H is *singular*.

1.2 Related work

The design of non-convex regularizers ensuring convexity of an objective function was proposed as part of the Graduated Non-Convexity (GNC) approach [9, 57, 59] and for binary image estimation [56]. Most methods

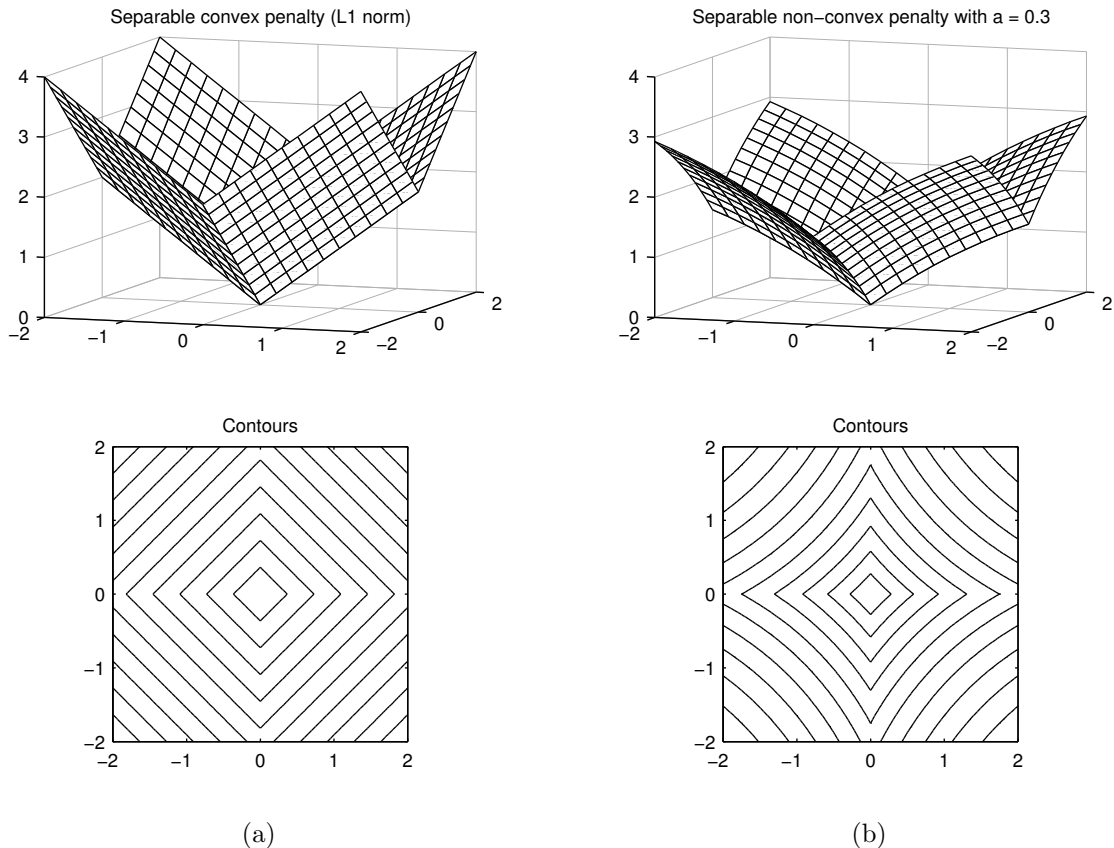


Figure 1: Separable bivariate penalties, convex and non-convex.

for non-convex sparse regularization do not aim to maintain convexity of the objective function. The ℓ_p pseudo-norm ($0 \leq p < 1$) is widely used, but other regularizers have also been advocated [16, 18, 38–40, 49, 50, 52, 53, 77, 81]. Several algorithms have been developed specifically for the ℓ_0 pseudo-norm: matching pursuit [51], greedy ℓ_1 [45], iterative hard thresholding and its variations [10, 35, 44, 64, 66, 78], smoothed ℓ_0 , [53], and single best replacement [74].

The penalty developed here is different from regularizers described in the literature, most of which are separable or are compositions of separable regularizers and linear operators. Non-separable penalties (e.g., mixed norms [4, 52, 72]) are generally used to capture statistical relationships among signal values (possibly linearly transformed¹) or to induce structured sparsity; they are not intended for unstructured, uncorrelated, ‘pure’ sparsity. Moreover, most sparsity-inducing penalties are neither parameterized nor utilized in the way undertaken here: namely, to induce sparsity subject to the constraint that the objective function is convex.

As the proposed method leads to a convex problem, convex sparse optimization methods may be used or adapted for its solution. Representative algorithms are the iterative shrinkage/thresholding algorithm (ISTA/FISTA) [8, 33], proximal methods [24, 25], alternating direction method of multipliers (ADMM) [2, 41], and majorization-minimization (MM) [32, 46].

Several algorithms are suitable for general non-convex sparse regularization problems, such as iteratively reweighted least squares (IRLS) [28, 42], iteratively reweighted ℓ_1 (IRL1) [3, 14, 79], FOCUSS [67], related algorithms [54, 55, 75], non-convex MM [23, 40, 50, 77], extensions of GNC [53, 57, 59], and other methods

¹Isotropic two-dimensional total variation, which induces joint sparsity of horizontal and vertical gradients, exemplifies this type of regularization.

Table 1: Penalties

$$\begin{aligned}
\phi(t; a) &= \frac{|t|}{1 + a|t|/2}, \quad a \geq 0 \\
\phi(t; a) &= \begin{cases} \frac{1}{a} \log(1 + a|t|), & a > 0 \\ |t|, & a = 0 \end{cases} \\
\phi(t; a) &= \begin{cases} \frac{2}{a\sqrt{3}} \left(\tan^{-1} \left(\frac{1+2a|t|}{\sqrt{3}} \right) - \frac{\pi}{6} \right), & a > 0 \\ |t|, & a = 0 \end{cases}
\end{aligned}$$

[15, 16, 38]. Non-convex regularization has also been used for blind deconvolution [68] and low-rank plus sparse matrix decompositions [17]. Convergence of these algorithms are generally to local optima only. However, conditions for convergence to a global minimizer, or to guarantee that all local minimizers are near a global minimizer, have been recently reported [20, 48]. Whereas Refs. [20, 48] focuses on convergence guarantees for given penalties, we focus on the design of penalties.

1.3 Notation

We write the vector $x \in \mathbb{R}^N$ as $x = (x_1, x_2, \dots, x_N)$. Given $x \in \mathbb{R}^N$, we define $x_n = 0$ for $n \notin \{1, 2, \dots, N\}$. (This simplifies expressions involving summations over n .) The ℓ_1 norm of $x \in \mathbb{R}^N$ is defined as $\|x\|_1 = \sum_n |x_n|$. If the matrix A is positive semidefinite, we write $A \succcurlyeq 0$. If the matrix $A - B$ is positive semidefinite, we write $A \succcurlyeq B$.

2 Univariate Penalties

The bivariate penalty to be given in Sec. 4 will be based on a parameterized non-convex univariate penalty function $\phi(\cdot; a): \mathbb{R} \rightarrow \mathbb{R}$ with parameter $a \geq 0$. We shall assume ϕ has the following properties:

- P1) $\phi(\cdot; a)$ is continuous on \mathbb{R}
- P2) $\phi(\cdot; a)$ is twice continuously differentiable, increasing, and concave on \mathbb{R}_+
- P3) $\phi(0; a) = 0$
- P4) $\phi(t; 0) = |t|$
- P5) $\phi(-t; a) = \phi(t; a)$
- P6) $\phi'(0^+; a) = 1$
- P7) $\phi''(0^+; a) = -a$
- P8) $\phi''(t; a) \geq -a$ for all $t \neq 0$
- P9) $\phi(t; a)$ is decreasing and convex in a .
- P10) $\phi(t; a) = (b/a) \phi(at/b; b)$ for $a, b > 0$ [Scaling].

It follows from symmetry that $\phi'(-t) = -\phi'(t)$ and $\phi''(-t) = \phi''(t)$. The scaling property of ϕ also induces a scaling property of ϕ' and ϕ'' . Namely,

$$\phi'(t; a) = \phi'(at/b; b), \quad (4)$$

$$\phi''(t; a) = (a/b) \phi''(at/b; b). \quad (5)$$

Table 1 lists several penalty functions that satisfy the above properties. For example, the rational [39], logarithmic, and arctangent functions [14, 58, 70] (when suitably normalized). The arctangent penalty is

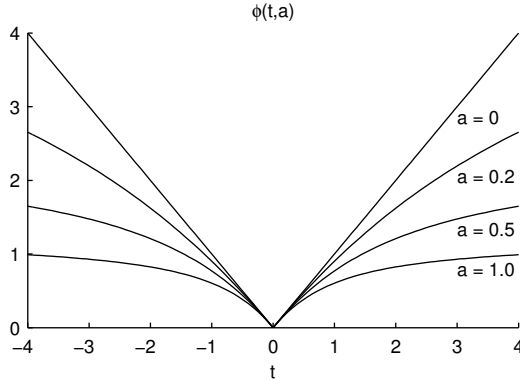


Figure 2: Penalty $\phi(t; a)$ for several values of a .

illustrated in Fig. 2 for several values of a . For larger a , the penalty functions increase more slowly, are more concave on the positive real line, and induce sparsity more strongly (i.e., by mildly penalizing large values). A comparison of the three penalties listed in Table 1 is illustrated in Figure 1 of Ref. [21] for a fixed value of a . Of the three penalties, the arctangent penalty increases the slowest for a fixed value of a .

We mention that we do not use the simpler form of the arctangent penalty, $\phi(t; a) = (1/a) \tan^{-1}(a|t|)$, as it does not satisfy $\phi''(0^+, a) = -a$ which is property P7 listed above.

Corresponding to a penalty ϕ having the above properties, we define a smooth concave function.

Definition 1. Let $\phi: \mathbb{R} \rightarrow \mathbb{R}$ be a penalty function satisfying the properties listed above. For $a \geq 0$, we define $s: \mathbb{R} \rightarrow \mathbb{R}$,

$$s(t; a) = \phi(t; a) - |t|. \quad (6)$$

Figure 3 illustrates the function s corresponding to the arctangent penalty for $a = 0.3$. The following proposition follows straightforwardly [62].

Proposition 1. Let $a \geq 0$. Let $\phi: \mathbb{R} \rightarrow \mathbb{R}$ be a penalty function satisfying the properties listed above. The function $s: \mathbb{R} \rightarrow \mathbb{R}$ in Definition 1 is twice continuously differentiable, concave, and satisfies

$$-a \leq s''(t; a) \leq 0. \quad (7)$$

This property will be of particular importance. Note that the value $\phi''(0)$ is not defined since ϕ is not differentiable at zero. But the value $s''(0)$ is defined (and is equal to $-a$).

$$s''(t; a) = \begin{cases} -a, & t = 0 \\ \phi''(t; a) & t \neq 0. \end{cases} \quad (8)$$

Also, although $\phi'(0)$ is not defined [because $\phi'(0^+) = 1$ and $\phi'(0^-) = -1$], the value $s'(0)$ is defined [$s'(0) = 0$]. Many of the properties listed above for ϕ are inherited by s , such as the symmetry and scaling properties:

$$s(-t; a) = s(t; a) \quad (9)$$

$$s(t; a) = (b/a) s(at/b; b) \quad (10)$$

$$s'(t; a) = s'(at/b; b) \quad (11)$$

$$s''(t; a) = (a/b) s''(at/b; b) \quad (12)$$

The following proposition is proven in Appendix A.1.

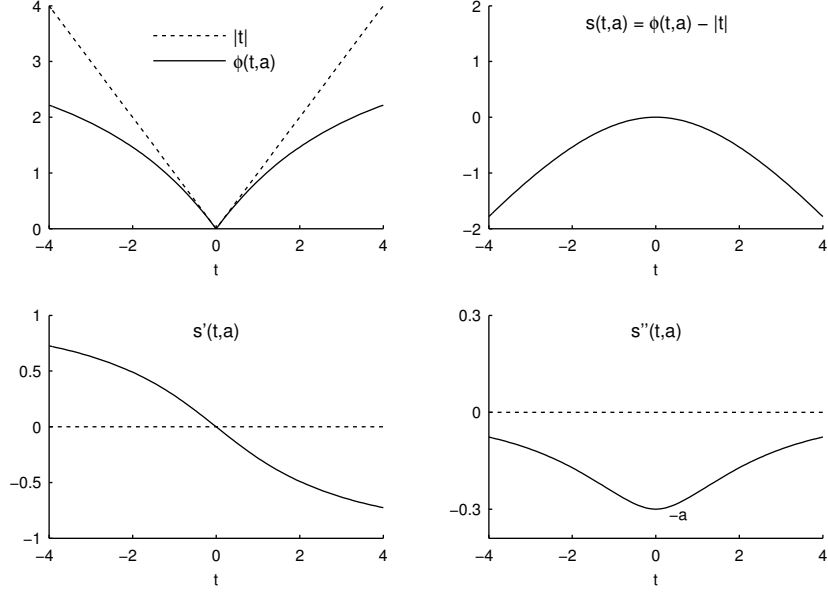


Figure 3: A univariate penalty ϕ , its corresponding function s , and the first and second-order derivatives of s . The function s is twice continuously differentiable and concave.

Proposition 2. Let $\phi: \mathbb{R} \rightarrow \mathbb{R}$ satisfy the properties listed above. Let $s: \mathbb{R} \rightarrow \mathbb{R}$ be given by Definition 1. Let $\lambda > 0$. If $0 \leq a \leq 1/\lambda$, then the functions $g: \mathbb{R} \rightarrow \mathbb{R}$

$$g(t) = \frac{1}{2}t^2 + \lambda s(t; a) \quad (13)$$

and $f: \mathbb{R} \rightarrow \mathbb{R}$

$$f(t) = \frac{1}{2}t^2 + \lambda \phi(t; a) \quad (14)$$

are convex functions.

3 Bivariate Concave Function

The bivariate penalty to be given in Sec. 4 will be defined in terms of a concave bivariate function S . The role of S , in describing the bivariate penalty, will be analogous to the role of s in describing the univariate penalty ϕ . Accordingly, the properties of S will be important for the properties of the bivariate penalty.

Definition 2. Let $a = (a_1, a_2)$ with $a_i \geq 0$. Let $\phi: \mathbb{R} \rightarrow \mathbb{R}$ be a univariate penalty function having the properties listed in Sec. 2. Let $s: \mathbb{R} \rightarrow \mathbb{R}$ be given by Definition 1. If at least one of $\{a_1, a_2\}$ is non-zero, we define the function $S: \mathbb{R}^2 \rightarrow \mathbb{R}$ as

$$S(x; a) = \begin{cases} s(x_1 + rx_2; \alpha) + (1-r)s(x_2; a_1), & x \in A_1 \\ s(rx_1 + x_2; \alpha) + (1-r)s(x_1; a_1), & x \in A_2 \\ s(rx_1 + x_2; \alpha) + (1+r)s(x_1; a_2), & x \in A_3 \\ s(x_1 + rx_2; \alpha) + (1+r)s(x_2; a_2), & x \in A_4 \end{cases}$$

where

$$\alpha = \frac{a_1 + a_2}{2}, \quad r = \frac{a_1 - a_2}{a_1 + a_2} \quad (15)$$

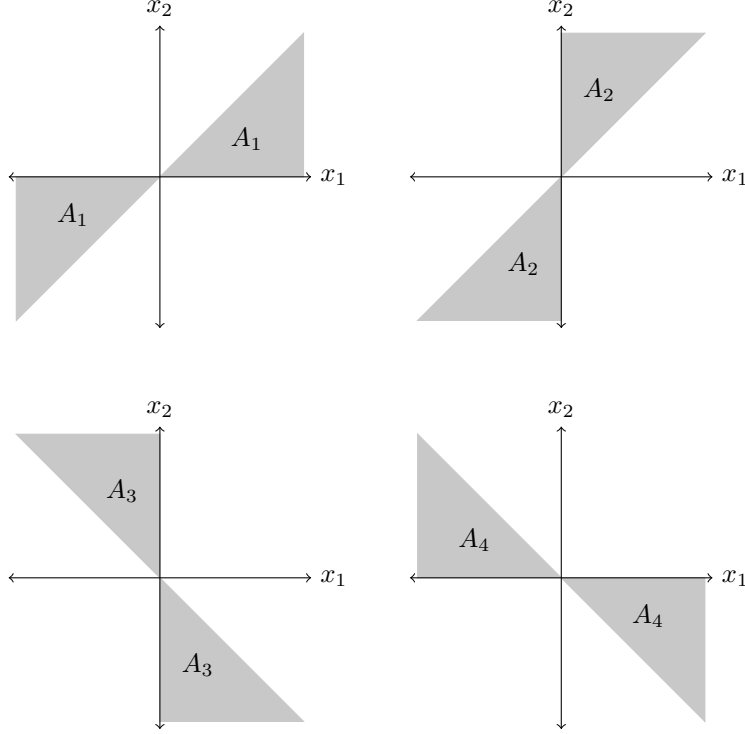


Figure 4: Regions A_1 through A_4 in Definition 2.

and sets $A_i \subset \mathbb{R}^2$ are

$$A_1 = \{x \in \mathbb{R}^2 \mid x_2(x_1 - x_2) \geq 0\} \quad (16)$$

$$A_2 = \{x \in \mathbb{R}^2 \mid x_1(x_1 - x_2) \leq 0\} \quad (17)$$

$$A_3 = \{x \in \mathbb{R}^2 \mid x_1(x_1 + x_2) \leq 0\} \quad (18)$$

$$A_4 = \{x \in \mathbb{R}^2 \mid x_2(x_1 + x_2) \leq 0\} \quad (19)$$

as shown in Fig. 4. If both $a_i = 0$, we define $S(x; 0) = 0$.

The non-negative parameters a_i characterize how strongly concave S is. Figure 5 illustrates S for the parameter values $a_1 = 1.5$ and $a_2 = 0.3$. The level sets of S are not ellipses, even though they appear ellipsoidal.

The function S has three symmetries:

$$S(x_1, x_2; a) = S(x_2, x_1; a) \quad (20a)$$

$$= S(-x_1, -x_2; a) \quad (20b)$$

$$= S(-x_2, -x_1; a) \quad (20c)$$

(any two of which imply the remaining one). Equivalently, S is symmetric with respect to the origin and the two lines $x_1 = x_2$ and $x_1 = -x_2$. These symmetries follow directly from Definition 2 and from the symmetry of the univariate function s .

The following lemmas are proven in the Appendix. It will be useful in the proofs to note some identities. First, note that $S(0; a) = 0$. From the definitions of α and r in (15), we have:

$$|r| \leq 1, \quad (1+r)\alpha = a_1 \quad (21)$$

$$r\alpha = (a_1 - a_2)/2, \quad (1-r)\alpha = a_2. \quad (22)$$

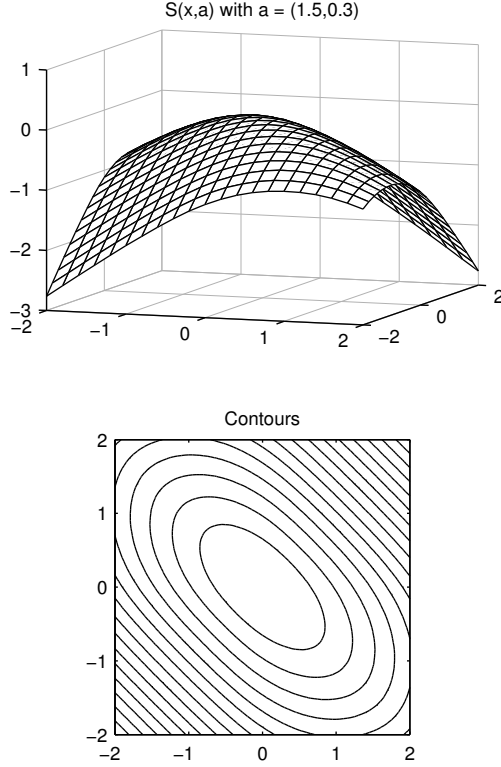


Figure 5: Non-separable concave function S in Definition 2.

Lemma 1. *The bivariate function $S: \mathbb{R}^2 \rightarrow \mathbb{R}$ in Definition 2 is twice continuously differentiable and concave on \mathbb{R}^2 .*

Lemma 2. *Let $a = (a_1, a_2)$ with $a_i \geq 0$. The Hessian of the bivariate function S in Definition 2 satisfies*

$$-\frac{1}{2} \begin{bmatrix} a_1 + a_2 & a_1 - a_2 \\ a_1 - a_2 & a_1 + a_2 \end{bmatrix} \preceq \nabla^2 S(x; a) \preceq 0, \quad \text{for all } x \in \mathbb{R}^2. \quad (23)$$

Equivalently,

$$-K(a) \preceq \nabla^2 S(x; a) \preceq 0, \quad \text{for all } x \in \mathbb{R}^2 \quad (24)$$

where $K(a)$ is defined by its eigenvalue decomposition

$$K(a) := Q^T \begin{bmatrix} a_1 & 0 \\ 0 & a_2 \end{bmatrix} Q = \frac{1}{2} \begin{bmatrix} a_1 + a_2 & a_1 - a_2 \\ a_1 - a_2 & a_1 + a_2 \end{bmatrix} \quad (25)$$

where Q is the orthonormal matrix defined in (3). Furthermore, the lower bound is attained at $x = 0$, i.e.,

$$\nabla^2 S(0; a) = -K(a). \quad (26)$$

Lemma 2 states that S is maximally concave at the origin. The lemma also gives the Hessian at the origin in terms of the parameters a_i . Lemma 2 is a key result for the subsequent results.

Lemma 2 can be illustrated in terms of ellipses. If M is a positive semidefinite matrix, then the set $\mathcal{E}[M] = \{x : x^T M^{-1} x \leq 1\}$ is an ellipsoid [11]. In addition, $M_1 \preceq M_2$ if and only if $\mathcal{E}[M_1] \subseteq \mathcal{E}[M_2]$. In

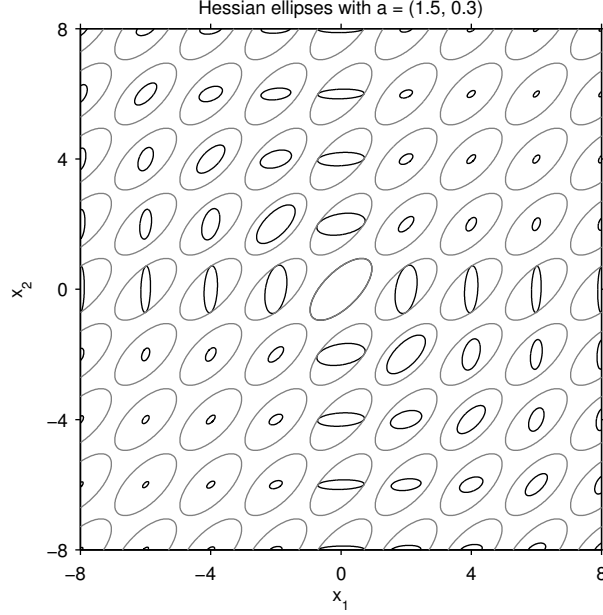


Figure 6: Illustration of Lemma 2. The black ellipses are inside the gray ellipses, indicating that $0.5x^\top Kx + S(x; a)$ is convex.

Fig. 6, we set $a_1 = 1.5$ and $a_2 = 0.3$. The ellipses corresponding to $K(a)$ and $-\nabla^2 S(x; a)$ are shown in gray and black, respectively. For each x , the black ellipse is contained within the gray ellipse, illustrating (24). For large x , the black ellipse shrinks, indicating that the function S becomes less concave away from the origin. The shrinkage behavior of the ellipse for large x_i is different in different quadrants: it shrinks faster in quadrants 1 and 3 than in quadrants 2 and 4. At $x = 0$, the black and gray ellipses coincide, reflecting the fact that the Hessian of S is equal to $-K(a)$ at the origin (26).

Theorem 1. Let $a = (a_1, a_2)$ with $a_i \geq 0$. Let $S: \mathbb{R}^2 \rightarrow \mathbb{R}$ be the function in Definition 2. Let $K(\gamma) = Q\Gamma Q^\top$ with eigenvalues $\gamma_i \geq 0$ be the positive semidefinite matrix defined in (2). The function $g: \mathbb{R}^2 \rightarrow \mathbb{R}$,

$$g(x; a, \gamma) = \frac{1}{2}x^\top K(\gamma)x + \lambda S(x; a), \quad \lambda > 0, \quad (27)$$

is convex if

$$0 \leq a_1 \leq \gamma_1/\lambda, \quad 0 \leq a_2 \leq \gamma_2/\lambda. \quad (28)$$

Proof. Since g is twice continuously differentiable, it is sufficient to show the Hessian of g is positive semidefinite. The Hessian of g is given by

$$\nabla^2 g(x; a, \gamma) = K(\gamma) + \lambda[\nabla^2 S(x; a)] \quad (29)$$

$$= Q^\top \Gamma Q + \lambda[\nabla^2 S(x; a)]. \quad (30)$$

From Lemma 2 it follows that

$$\nabla^2 g(x; a, \gamma) \succeq Q^\top \begin{bmatrix} \gamma_1 - \lambda a_1 & 0 \\ 0 & \gamma_2 - \lambda a_2 \end{bmatrix} Q. \quad (31)$$

Hence, $g(x; a, \gamma)$ is convex if $\gamma_i - \lambda a_i \geq 0$ for $i = 1, 2$. This proves the result. \square

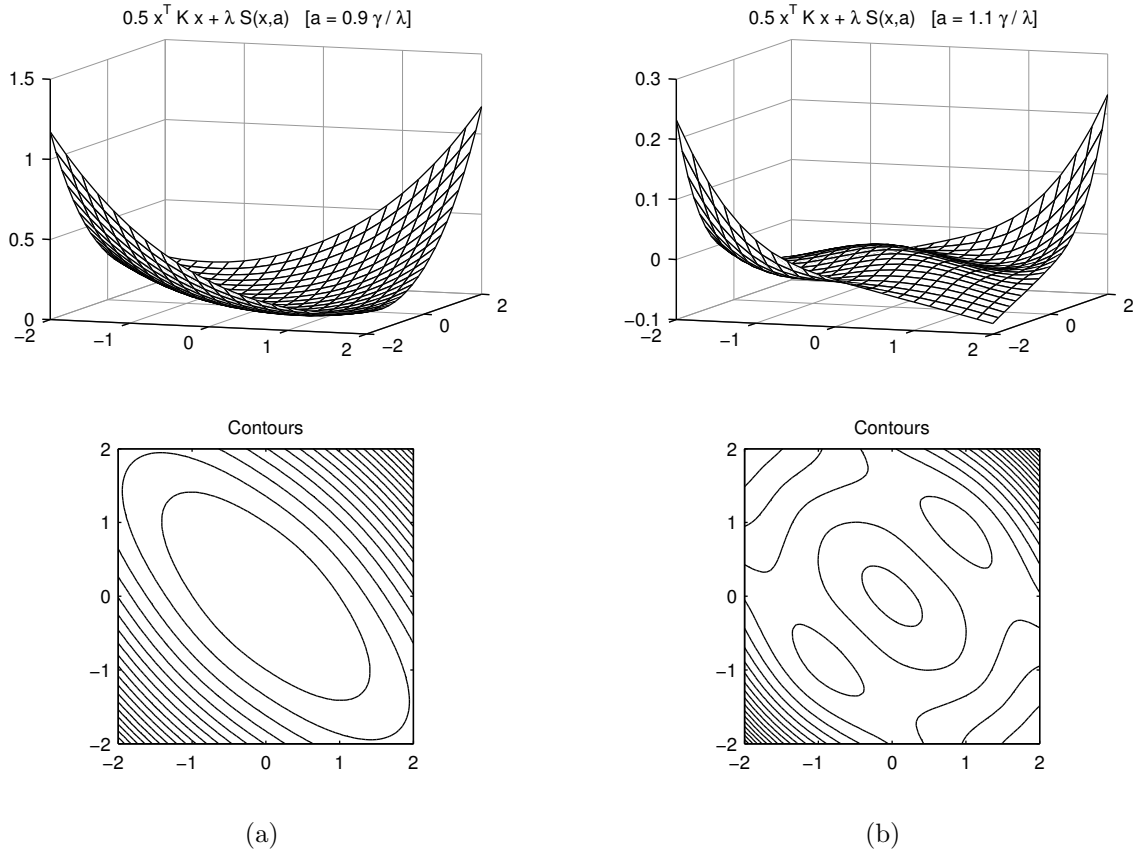


Figure 7: Illustration of convexity condition (28). (a) Function g is convex as a_i satisfy (28). (b) Function g is not convex as a_i violate (28).

Theorem 1 is illustrated in Fig. 7. In this example, we set $\gamma_1 = 1.5$, $\gamma_2 = 0.3$, and $\lambda = 15.0$. Hence, the critical parameters are $a_1^* = \gamma_1/\lambda = 0.1$ and $a_2^* = \gamma_2/\lambda = 0.02$. If either a_1 or a_2 is greater than the respective critical value, then the function g in (27) will be non-convex. In Fig. 7(a), we set $a_i = 0.9\gamma_i/\lambda < a_i^*$ to satisfy condition (28), hence g is convex. In contrast, in Fig. 7(b), we set $a_i = 1.1\gamma_i/\lambda > a_i^*$ violating condition (28), hence g is non-convex. The lack of convexity can be recognized in both the surface and contour plots.

4 Bivariate Penalties

In this section, we define a non-convex non-separable bivariate penalty. Our intention is to strongly induce sparsity in solutions of problem (1) while maintaining the convexity of the problem. The penalty is parameterized by two non-negative parameters a_1 and a_2 , which we restrict so as to ensure convexity of the objective function.

Definition 3. Let $a = (a_1, a_2)$ with $a_i \geq 0$. Let $\phi: \mathbb{R} \rightarrow \mathbb{R}$ be a univariate penalty function having the properties listed in Sec. 2. Let $S: \mathbb{R}^2 \rightarrow \mathbb{R}$ be the corresponding function in Definition 2. We define the bivariate penalty function $\psi: \mathbb{R}^2 \rightarrow \mathbb{R}$ as

$$\psi(x; a) = S(x; a) + \|x\|_1. \quad (32)$$

If $a_1 \neq a_2$, then the penalty ψ is non-separable. Figure 8 illustrates ψ for the parameter values $a_1 = 1.5$ and $a_2 = 0.3$. The degree of non-convexity differs in different quadrants. Note in Fig. 8 that the contours

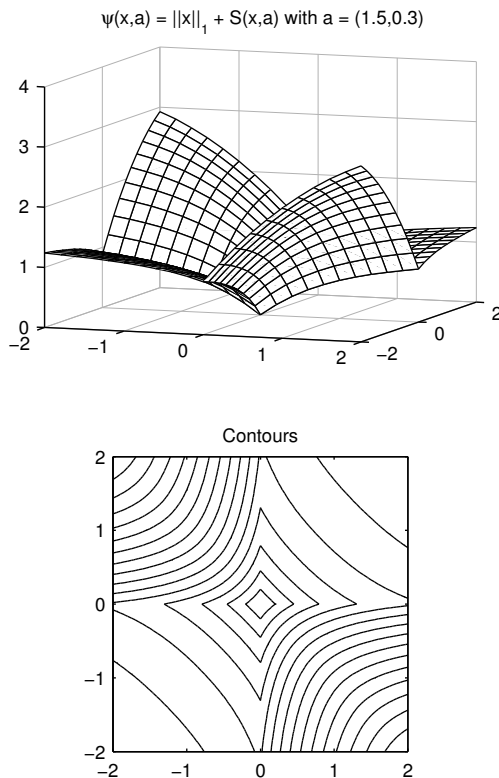


Figure 8: Non-separable non-convex penalty ψ in Definition 3.

of ψ resemble those of the separable non-convex penalty in Fig. 1, but the curvature is more pronounced in quadrants 2 and 4 and less pronounced in quadrants 1 and 3. The parameters a_1 and a_2 determine the precise behavior of the penalty.

It is informative to consider special cases of the bivariate penalty. If $a_1 > 0$ and $a_2 = 0$, then ψ simplifies to

$$\psi(x) = |x_1| + |x_2| + \phi(x_1 + x_2; a_1/2) - |x_1 + x_2|. \quad (33)$$

If $a_1 = a_2$, then the penalty reduces to a separable function, $\psi(x) = \phi(x_1; a_1) + \phi(x_2; a_1)$ (see Fig. 1(b)). If $a_1 = a_2 = 0$, then it further reduces to the ℓ_1 norm, i.e., $\psi(x) = |x_1| + |x_2|$ (see Fig. 1(a)). In any case, if either a_1 or a_2 is positive, then ψ is non-convex.

The following theorem, based on Theorem 1, states how to restrict the parameters a_i to ensure problem (1) is convex.

Theorem 2. *Let $\psi: \mathbb{R}^2 \rightarrow \mathbb{R}$ be the bivariate penalty in Definition 3. Suppose $H^\top H = Q^\top \Gamma Q$ where Q and Γ are given by (3). If $a = (a_1, a_2)$ satisfy $0 \leq a_i \leq \gamma_i/\lambda$, then the bivariate objective function $f := \mathbb{R}^2 \rightarrow \mathbb{R}$,*

$$f(x; a) = \frac{1}{2} \|y - Hx\|_2^2 + \lambda \psi(x; a), \quad (34)$$

is convex.

Proof. We write

$$f(x; a) = g(x; a) + \frac{1}{2} y^\top y - y^\top Hx + \lambda \|x\|_1 \quad (35)$$

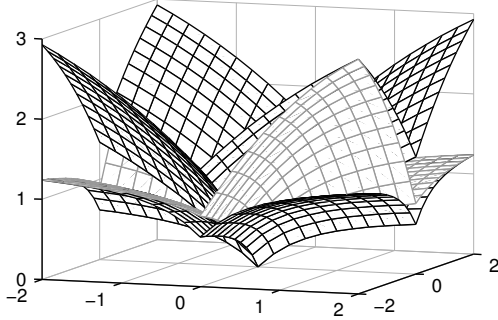


Figure 9: Illustration of Theorem 3. The non-separable penalty ψ lies between two separable penalties.

where g is given by (27) with $K = H^T H$ therein. From Theorem 1, g is convex. Hence, f is convex because it is the sum of convex functions. \square

Theorem 2 gives a range for parameters a_1 and a_2 to ensure the objective function f is convex. Precisely, the parameters should be bounded, respectively, by the eigenvalues of $(1/\lambda)H^T H$. To maximally induce sparsity, the parameters should be set to the maximal (critical) values, $a_i = \gamma_i/\lambda$.

Note that, even when the matrix H is singular (i.e., $\gamma_1 = 0$ or $\gamma_2 = 0$), the bivariate penalty can be non-convex without spoiling the convexity of the objective function f (if at least one of γ_i is positive). In other words, we need *not* sacrifice the convexity of the objective function f in order to use sparsity-inducing non-convex penalties, even when H is *singular*. This is an impossibility when the penalty ψ is a separable function.

Other bivariate penalties can be defined that ensure the objective function is convex; however, the one defined here satisfies a further property we think should be required of a bivariate penalty. Namely, the proposed bivariate penalty lies between the two separable penalties corresponding to the minimum and maximum parameters a_i .

Theorem 3. *Let $a = (a_1, a_2)$ with $a_i \geq 0$. Set $a_{\min} = \min\{a_1, a_2\}$ and $a_{\max} = \max\{a_1, a_2\}$. The bivariate penalty ψ in Definition 3 satisfies*

$$\phi(x_1; a_{\max}) + \phi(x_2; a_{\max}) \leq \psi(x; a) \leq \phi(x_1; a_{\min}) + \phi(x_2; a_{\min}). \quad (36)$$

The theorem is proven in Appendix A.6. (The supplemental material has an animated illustration of these bounds.)

The inequality in Theorem 3 is tight: the lower and upper bounds are individually satisfied with equality on the lines $\{x = (t, t)\}$ and $\{x = (t, -t)\}$, as illustrated in Fig. 9. Note that when $a_1 = a_2$ (i.e., $a_{\min} = a_{\max}$), the theorem requires the penalty ψ to be separable. Indeed, the penalty (32) is separable when $a_1 = a_2$.

We think a bivariate penalty should satisfy the inequality of Theorem 3 for the following reason. In this work, we aim to induce pure sparsity (i.e., not structured sparsity, etc.). Therefore, when $H^T H$ is a diagonal matrix we should use a separable penalty. (A separable penalty best reflects an iid prior.) It follows that when $H^T H = \gamma_1 I$, the most suitable penalty (maintaining convexity of f) is the separable one: $\phi(x_1, \gamma_1/\lambda) + \phi(x_2, \gamma_1/\lambda)$. A parameterized bivariate penalty should recover this separable penalty as a special case. Moreover, if $H^T H = \gamma_2 I$ with $\gamma_2 < \gamma_1$, then the most suitable penalty is again a separable one: $\phi(x_1, \gamma_2/\lambda) + \phi(x_2, \gamma_2/\lambda)$. But $\gamma_2 < \gamma_1$ means the corresponding data fidelity term is less strongly convex and thus the penalty term must be less strongly non-convex. Consequently, we must have

$$\phi(x_1, \gamma_1/\lambda) + \phi(x_2, \gamma_1/\lambda) < \phi(x_1, \gamma_2/\lambda) + \phi(x_2, \gamma_2/\lambda).$$

When $H^\top H$ has distinct eigenvalues γ_1 and γ_2 , the most suitable bivariate penalty should lie between these two separable penalties. Theorem 3 assures this.

If not suitably designed and utilized, it is conceivable that a non-separable penalty may lead to correlation or structure in the estimated signal that is not present in original sparse signal. To avoid unintentionally inducing correlation in the estimated signal, it seems reasonable that the bivariate penalty should exhibit some similarity to the corresponding separable penalties (that reflect unstructured sparsity). Theorem 3 indicates the bivariate penalty (32) conforms to the relevant separable penalties. It is still possible that some erroneous correlation might be introduced, but such correlation is not evident in the experimental results. We attribute this to Theorem 3.

One may question the legitimacy of a method wherein penalty parameters are set according to the data fidelity term. Conventionally, the penalty term should reflect prior knowledge of the signal to be estimated; it should not depend on H , which represents the observation model. (This is formalized in the Bayesian perspective where the objective function corresponds to a likelihood function and the penalty term corresponds to a prior). The approach taken here, wherein the parameters of the penalty term are based on properties of H , appears to violate this principle. However, the common practice of restricting the penalty to be convex also violates this principle. Probability densities (e.g., generalized Gaussian [51], mixture models [22, 65], Bessel-K [31], and α -stable [1]), that accurately model sparsity, correspond to non-convex penalties. Using the ℓ_1 norm as a penalty corresponds to the Laplace distribution (a relatively weak sparsity model). The proposed bivariate sparse regularization (BISR) approach is simply intended to follow a sparsity prior more closely.

4.1 Separable penalties

To clarify the value of non-separable regularization, we note a limitation of separable penalties.

Lemma 3. *Let the univariate penalty $\phi: \mathbb{R} \rightarrow \mathbb{R}$ satisfy the properties of Sec. 2. The objective function $f: \mathbb{R}^2 \rightarrow \mathbb{R}$,*

$$f(x; a) = \frac{1}{2} \|y - Hx\|_2^2 + \lambda \phi(x_1; a) + \lambda \phi(x_2; a), \quad (37)$$

with $\lambda > 0$ and $a \geq 0$, is convex only if

$$\phi''(0^+) \geq -(1/\lambda) \min\{\gamma_1, \gamma_2\}, \quad (38)$$

or equivalently, $0 \leq a \leq \min\{\gamma_1, \gamma_2\}/\lambda$, where γ_i are the eigenvalues of $H^\top H$.

Proof. Let $u \in \mathbb{R}^2$ be an eigenvector of $H^\top H$ corresponding to its minimum eigenvalue γ_{\min} , i.e.,

$$H^\top H u = \gamma_{\min} u. \quad (39)$$

Consider f on a line in the direction of u . Namely, define $g: \mathbb{R} \rightarrow \mathbb{R}$ as

$$g(t) = f(tu; a) \quad (40)$$

$$= \frac{1}{2} \|y - tHu\|_2^2 + \lambda \phi(tu_1; a) + \lambda \phi(tu_2; a). \quad (41)$$

We will show that g is not convex when $a > \gamma_{\min}$. It will follow that f is not convex, because the restriction of a multivariate convex function to any line must also be convex.

By the properties of ϕ , the function g is twice continuously differentiable on \mathbb{R}_+ and its second derivative is given by

$$g''(t) = uH^\top H u + \lambda u_1^2 \phi''(tu_1; a) + \lambda u_2^2 \phi''(tu_2; a) \quad (42)$$

$$= \gamma_{\min} u^\top u + \lambda u_1^2 \phi''(tu_1; a) + \lambda u_2^2 \phi''(tu_2; a). \quad (43)$$

Since $\phi''(0^+; a) = -a$ is a defining property of ϕ , we have

$$g''(0^+) = \gamma_{\min} u^\top u - \lambda u_1^2 a - \lambda u_2^2 a \quad (44)$$

$$= (\gamma_{\min} - \lambda a) u^\top u. \quad (45)$$

Hence, convexity of g requires $\gamma_{\min} - \lambda a \geq 0$; i.e., $a \leq \gamma_{\min}/\lambda$. \square

According to Lemma 3, a *separable* non-convex penalty, that ensures convexity of the objective function, is limited by the minimum eigenvalue of $H^\top H$. It cannot exploit the greater eigenvalue. This is unfavorable, because when one of the eigenvalues is close to zero, a separable penalty can be only mildly non-convex and provides negligible improvement relative to the ℓ_1 norm; when $H^\top H$ is singular, we recover the ℓ_1 norm. In contrast, a non-separable penalty can exploit both eigenvalues independently. Hence, non-separable penalties are most advantageous when the eigenvalues of $H^\top H$ are quite different in value.

5 Sparse Reconstruction

Practical problems in signal processing involve far more than two variables. Therefore, the proposed bivariate penalty (32) and convexity condition (28) are of little practical use on their own. In this section we show how they can be used to solve an N -point linear inverse problem (with $N > 2$). We consider the problem of estimating a signal $x \in \mathbb{R}^N$ given y ,

$$y = Hx + w \quad (46)$$

where H is a known linear operator, x is known to be sparse, and w is additive white Gaussian noise (AWGN). We formulate the estimation of x as an optimization problem with bivariate sparse regularization (BISR),

$$\hat{x} = \arg \min_{x \in \mathbb{R}^N} \left\{ F(x) = \frac{1}{2} \|y - Hx\|_2^2 + \frac{\lambda}{2} \sum_n \psi((x_{n-1}, x_n); a) \right\}, \quad \lambda > 0 \quad (47)$$

where $a = (a_1, a_2)$ and $\psi: \mathbb{R}^2 \rightarrow \mathbb{R}$ is the proposed bivariate penalty (32). In the penalty term, the first and last signal values pairs, (x_0, x_1) and (x_N, x_{N+1}) , straddle the end-points of x . As noted in Sec. 1.3, we define $x_n = 0$ for $n \notin \{1, 2, \dots, N\}$, which simplifies subsequent notation.

If $a_1 = a_2$, then the bivariate penalty is separable, i.e., $\psi(u; a) = \phi(u_1; a_1) + \phi(u_2; a_1)$, and the N -point penalty term in (47) reduces to $\lambda \sum_n \phi(x_n, a_1)$. Hence, we recover the standard (separable) formulation of sparse regularization. In particular, if $a_1 = a_2 = 0$, then $\psi(u; 0) = |u_1| + |u_2|$ and the N -point penalty term reduces to $\lambda \|x\|_1$, i.e., the classical sparsity-inducing convex penalty.

In order to induce sparsity more effectively, we allow ψ to be non-separable; i.e., $a_1 \neq a_2$. To that end, the following section addresses the problem of how to set a_1 and a_2 in the bivariate penalty ψ to ensure convexity of the N -variate objective function F in (47).

5.1 Convexity condition

Lemma 4. *Let $F: \mathbb{R}^N \rightarrow \mathbb{R}$ be defined in (47) where $\psi: \mathbb{R}^2 \rightarrow \mathbb{R}$ is a parameterized bivariate penalty as defined in Definition 3. Let P be a positive semidefinite symmetric tridiagonal Toeplitz matrix,*

$$P = \begin{bmatrix} p_0 & p_1 & & & \\ p_1 & p_0 & p_1 & & \\ & \ddots & \ddots & \ddots & \\ & & p_1 & p_0 & p_1 \\ & & & p_1 & p_0 \end{bmatrix}, \quad (48)$$

such that $0 \preceq P \preceq H^\top H$. If the bivariate function $f: \mathbb{R}^2 \rightarrow \mathbb{R}$ defined as

$$f(u) = \frac{1}{2} u^\top \begin{bmatrix} p_0 & 2p_1 \\ 2p_1 & p_0 \end{bmatrix} u + \lambda \psi(u; a) \quad (49)$$

is convex, then F is convex.

The lemma is proven in Appendix A.7. According to the lemma, it is sufficient to restrict ψ so as to ensure convexity of the bivariate function f in (49). Therefore, the allowed penalty parameters a_i can be determined from the tridiagonal matrix P . Using Theorem 1 and Lemma 4, we obtain Theorem 4.

Theorem 4. Let $F: \mathbb{R}^N \rightarrow \mathbb{R}$ be defined in (47) where $\psi: \mathbb{R}^2 \rightarrow \mathbb{R}$ is a parameterized bivariate penalty as defined in Definition 3. Let P be a symmetric tridiagonal Toeplitz matrix (48) satisfying $0 \preceq P \preceq H^\top H$. If

$$0 \leq a_1 \leq (p_0 + 2p_1)/\lambda, \quad 0 \leq a_2 \leq (p_0 - 2p_1)/\lambda, \quad (50)$$

then F in (47) is convex.

Proof. Note the eigenvalue value decomposition

$$\begin{bmatrix} p_0 & 2p_1 \\ 2p_1 & p_0 \end{bmatrix} = Q^\top \begin{bmatrix} p_0 + 2p_1 & 0 \\ 0 & p_0 - 2p_1 \end{bmatrix} Q \quad (51)$$

where Q is the orthonormal matrix (3). Hence, f in (49) can be written as

$$f(u) = \frac{1}{2} u^\top Q^\top \begin{bmatrix} p_0 + 2p_1 & 0 \\ 0 & p_0 - 2p_1 \end{bmatrix} Q u + \lambda \psi(u; a). \quad (52)$$

By Theorem 1, if $0 \leq a_1 \leq (p_0 + 2p_1)/\lambda$ and $0 \leq a_2 \leq (p_0 - 2p_1)/\lambda$, then f is convex. It follows from Lemma 4 that F in (47) is convex. \square

5.2 Optimality condition

In this section, we derive an explicit condition to verify the optimality of a prospective minimizer of the objective function F in (47). The optimality condition is also useful for monitoring the convergence of an optimization algorithm (see the animation in the supplemental material).

The general condition to characterize minimizers of a convex function is expressed in terms of the subdifferential. If F is convex, then $x^{\text{opt}} \in \mathbb{R}^N$ is a minimizer if and only if $0 \in \partial F(x^{\text{opt}})$ where ∂F is the subdifferential of F .

We seek an expression for the subdifferential of the objective function F . The function F in (47) has a regularization term that is non-differentiable, non-convex, and non-separable. But with the aid of (32), we may write the regularization term as:

$$\frac{1}{2} \sum_n \psi((x_{n-1}, x_n); a) = \frac{1}{2} \sum_n \left[S((x_{n-1}, x_n); a) + \|(x_{n-1}, x_n)\|_1 \right] \quad (53)$$

$$= \frac{1}{2} \sum_n \left[S((x_{n-1}, x_n); a) + |x_{n-1}| + |x_n| \right] \quad (54)$$

$$= \|x\|_1 + \frac{1}{2} \sum_n S((x_{n-1}, x_n); a) \quad (55)$$

where $x_n = 0$ for $n \notin \{1, 2, \dots, N\}$. We define $\Theta: \mathbb{R}^N \rightarrow \mathbb{R}$ as

$$\Theta(x; a) = \frac{1}{2} \sum_n S((x_{n-1}, x_n); a). \quad (56)$$

The function Θ is differentiable, it being the sum of differentiable functions. Using (55), we may express the objective function F in (47) as

$$F(x) = \frac{1}{2}\|y - Hx\|_2^2 + \lambda\Theta(x; a) + \lambda\|x\|_1. \quad (57)$$

The benefit of (57) compared to (47) is that the regularization term (which is non-differentiable, non-convex, and non-separable) is separated into a differentiable part and a convex separable part. The Θ term is differentiable and its gradient is easily evaluated. The ℓ_1 norm is separable and convex and its subdifferential is easily evaluated.

The gradient of Θ is given by

$$[\nabla\Theta(x; a)]_n = \frac{1}{2}S_1((x_n, x_{n+1}); a) + \frac{1}{2}S_2((x_{n-1}, x_n); a) \quad (58)$$

where S_i is the partial derivative of $S((x_1, x_2))$ with respect to x_i . They are tabulated in (85) and (86).

The subdifferential of the ℓ_1 norm is separable [11],

$$\partial\|x\|_1 = \text{sign}(x_1) \times \cdots \times \text{sign}(x_N) \quad (59)$$

where sign is the set-valued signum function

$$\text{sign}(t) := \begin{cases} \{1\}, & t > 0 \\ [-1, 1], & t = 0 \\ \{-1\}, & t < 0. \end{cases} \quad (60)$$

Since the first two terms of (57) are differentiable, the subdifferential of F is

$$\partial F(x) = H^\top(Hx - y) + \lambda\nabla\Theta(x; a) + \lambda\partial\|x\|_1. \quad (61)$$

Hence the condition $0 \in \partial F(x^{\text{opt}})$ can be expressed as

$$(1/\lambda)H^\top(y - Hx^{\text{opt}}) - \nabla\Theta(x^{\text{opt}}; a) \in \partial\|x^{\text{opt}}\|_1. \quad (62)$$

Expressing this condition component-wise, we have the following result.

Theorem 5. *If $a = (a_1, a_2)$ is chosen so that the objective function F in (47) is convex, then x^{opt} minimizes F if and only if*

$$\frac{1}{\lambda}[H^\top(y - Hx^{\text{opt}})]_n - [\nabla\Theta(x^{\text{opt}}; a)]_n \in \text{sign}(x_n^{\text{opt}}), \quad n = 1, \dots, N. \quad (63)$$

This condition can be depicted using a scatter plot as in Fig. 14 below. The points in the scatter plot show the left-hand-side of (63) versus x_n for $n = 1, \dots, N$. A signal x^{opt} is a minimizer of F if and only if the points in the scatter plot lie on the graph of the set-valued signum function (e.g., Fig. 14).

5.3 Sparse Deconvolution

We apply Theorem 4 to the sparse deconvolution problem. In this case, the linear operator H represents convolution, i.e.,

$$[Hx]_n = \sum_k h_{n-k} x_k. \quad (64)$$

That is, H is a Toeplitz matrix. It represents a linear time-invariant (LTI) system with frequency response given by the Fourier transform of h ,

$$H(\omega) = \sum_n h_n e^{-j\omega n}. \quad (65)$$

Similarly, the matrix P in (48) represents an LTI system with a real-valued frequency response,

$$P(\omega) = p_1 e^{-j\omega} + p_0 + p_1 e^{j\omega} \quad (66)$$

$$= p_0 + 2p_1 \cos(\omega). \quad (67)$$

Specializing Theorem 4 to the problem of deconvolution, we have the following result.

Theorem 6. *Let H in (47) represent convolution. Let P in (67) satisfy*

$$0 \leq P(\omega) \leq |H(\omega)|^2, \quad \forall \omega, \quad (68)$$

where $H(\omega)$ is given by (65). If $0 \leq a_1 \leq P(0)/\lambda$ and $0 \leq a_2 \leq P(\pi)/\lambda$, then F in (47) is convex.

Proof. Using the convolution property of the discrete-time Fourier transform, condition (68) is equivalent to $0 \preceq P_\infty \preceq H_\infty^\top H_\infty$, where these are doubly-infinite Toeplitz matrices corresponding to discrete-time signals defined on \mathbb{Z} . Since any principal sub-matrix of a positive semidefinite matrix is also positive semidefinite, the inequality is also true for finite matrices P and $H^\top H$, which can be recognized as principal sub-matrices of the corresponding doubly-infinite matrices. Therefore, $0 \preceq P \preceq H^\top H$, and by Theorem 4, the objective function F is convex if a_i satisfy (50). Noting that $P(0) = p_0 + 2p_1$ and $P(\pi) = p_0 - 2p_1$ yields the result. \square

To induce sparsity as strongly as possible, $P(\omega)$ should be as close as possible to the upper bound $|H(\omega)|^2$. The determination of $P(\omega)$ satisfying such constraints can be efficiently and exactly performed using semi-definite programming (SDP) as described by Dumitrescu [30]. Since P is low-order here, the SDP computation is negligible.

An example is illustrated in Fig. 10. The impulse response h is shown in Fig. 10(a). The square magnitude of the frequency response $|H(\omega)|^2$ is shown in Fig. 10(b). The frequency response $P(\omega) = 0.4 + 0.2 \cos(\omega)$ is real-valued, non-negative, and approximates $|H(\omega)|^2$ from below. According to Theorem 6, the objective function F is convex if $0 \leq a_1 \leq 0.6/\lambda$ and $0 \leq a_2 \leq 0.2/\lambda$. This filter will be used in Example 1 below (Sec. 7.1).

Another example is illustrated in Fig. 11. The frequency response $H(\omega)$ has a null at $\omega = \pi$. Hence, the system H is not invertible. Since $H(\pi) = 0$, any P satisfying (68) also has $P(\pi) = 0$. We find $P(\omega) = 0.38(1 + \cos \omega)$ satisfies (68); see Fig. 11(b). Therefore, according to Theorem 6, the objective function F is convex if $0 \leq a_1 \leq 0.76/\lambda$ and $a_2 = 0$. For $\{a_1 > 0, a_2 = 0\}$, the multivariate penalty is non-convex and non-separable. For $\{a_1 = a_2 = 0\}$, the penalty is simply the ℓ_1 norm (convex and separable). This filter will be used in Example 2 below (Sec. 7.2).

In reference to the filters H illustrated in Figs. 10 and 11, it is informative to consider the case of a separable penalty. If ψ is a separable penalty (i.e., $a_1 = a_2$), then the objective function F is convex only if $0 \leq a_1 = a_2 \leq \min_\omega |H(\omega)|^2$. For the filter of Fig. 10 this leads to the constraint $0 \leq a_1 = a_2 \leq 0.26$, meaning that the separable penalty may be non-convex (i.e., $a_1 = a_2 > 0$ is allowed). On the other hand, for the filter of Fig. 11 this leads to the constraint $a_1 = a_2 = 0$, i.e., $\psi(x, a) = |x_1| + |x_2|$. When the filter H is not invertible, the only non-convex penalties maintaining convexity of the objective function F are *non-separable* penalties. Since inverse problems often involve singular or nearly singular operators H , this motivates the development of non-separable penalties as herein.

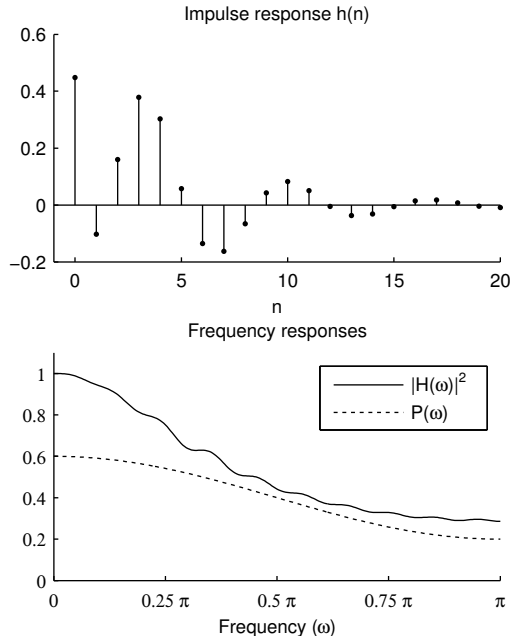


Figure 10: Filters $H(\omega)$ and $P(\omega)$ for Example 1.

6 Algorithms

6.1 Iterative L1 minimization

We present an iterative L1 norm minimization algorithm to solve (47). The derivation is based on majorization-minimization (MM) [32]. The MM principle consists of the iteration

$$x^{(k+1)} \in \arg \min_x F^M(x; x^{(k)}) \quad (69)$$

where k is the iteration index and F^M denotes a majorizer of the objective function F , i.e.,

$$F^M(x; v) \geq F(x), \quad \text{for all } x, v \quad (70)$$

$$F^M(v; v) = F(v), \quad \text{for all } v. \quad (71)$$

The function $S: \mathbb{R}^2 \rightarrow \mathbb{R}$ defined in Lemma 1 is twice continuously differentiable and concave. Therefore, a majorizer of S is given by

$$S^M(x; v) = S(v) + [\nabla S(v)]^T(x - v) \quad (72)$$

where ∇S is the gradient of S . See Fig. 12. The majorizer $S^M(x; v)$ is linear in x ; hence convex in x . A majorizer of the bivariate penalty ψ is then obtained using (32),

$$\psi^M(x; v) = S^M(x; v) + \|x\|_1 \quad (73)$$

$$= S(v) + [\nabla S(v)]^T(x - v) + \|x\|_1. \quad (74)$$

The majorizer $\psi^M(x; v)$ is convex in x , it being a sum of convex functions.

Recall the objective function F in (47) can be expressed as (57). Therefore, a majorizer of the objective function F in (47) is given by

$$F^M(x; v) = \frac{1}{2} \|y - Hx\|_2^2 + \lambda \Theta^M(x; v; a) + \lambda \|x\|_1 \quad (75)$$

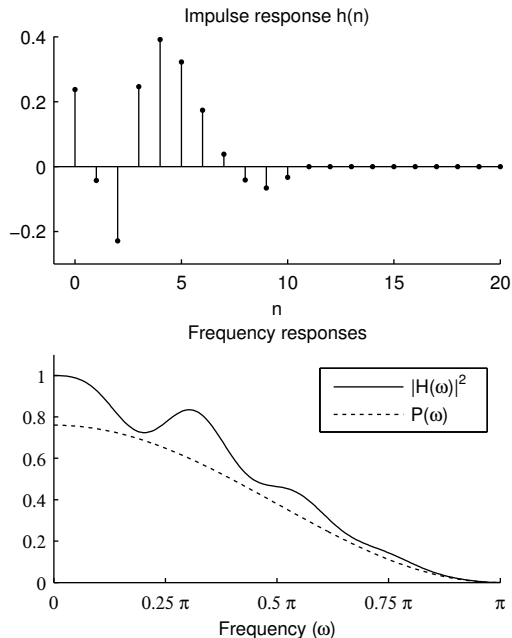


Figure 11: Filters $H(\omega)$ and $P(\omega)$ for Example 2.

where $\Theta^M(x; v; a)$ is a majorizer of $\Theta(x; a)$. We recall the bivariate function S is concave and twice continuously differentiable. Therefore, the N -variate function Θ is concave as it is a sum of concave functions. Likewise, Θ is twice continuously differentiable. Therefore, a majorizer of Θ is given by

$$\Theta^M(x; v; a) = \Theta(v; a) + [\nabla\Theta(v; a)]^T(x - v) \quad (76)$$

where $\nabla\Theta$ is given by (58). Hence, F^M is given by

$$F^M(x; v) = \frac{1}{2}\|y - Hx\|_2^2 + \lambda[\nabla\Theta(v; a)]^T x + \lambda\|x\|_1 + C(v) \quad (77)$$

where $C(v)$ does not depend on x . The MM iteration (69) is then given by

$$x^{(k+1)} \in \arg \min_{x \in \mathbb{R}^N} \left\{ \frac{1}{2}\|y - Hx\|_2^2 + \lambda[\nabla\Theta(x^{(k)}; a)]^T x + \lambda\|x\|_1 \right\}. \quad (78)$$

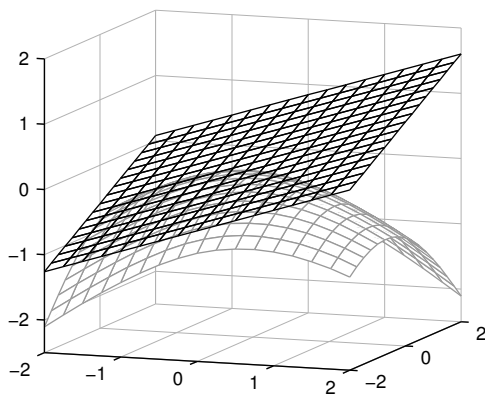


Figure 12: Majorization of concave function S by linear function S^M .

This is a standard ℓ_1 norm optimization problem which can be solved by several methods (e.g. proximal methods, ADMM). Hence, the solution to (47) can be obtained by iterative ℓ_1 norm minimization.

Based on the theory of MM algorithms, it is guaranteed that $x^{(k)}$ converges to the minimizer of F when F is strictly convex [13, 43]. If H is not invertible, then F may be convex without being strictly convex. In this case: (a) the function value $F(x^{(k)})$ converges to the minimum value of F , and (b) if F has a unique minimizer, then $x^{(k)}$ converges to it. See Theorems 4.1 and 4.4 of [43].

6.2 Iterative thresholding

We present an iterative thresholding algorithm to solve (47). The algorithm is an immediate application of forward-backward splitting (FBS) [25, 26]. The FBS algorithm minimizes a function of the form $f_1 + f_2$ where both f_1 and f_2 are convex and additionally ∇f_1 is Lipschitz continuous. To apply the FBS algorithm to problem (47), we express F using (57). The first two terms of (57) constitute the smooth convex function f_1 . We remark that since Θ is concave, the Lipschitz constant of ∇f_1 is bounded by ρ where ρ is the maximum eigenvalue of $H^T H$. The ℓ_1 norm term in (57) constitutes the (non-smooth) convex function f_2 . An FBS algorithm to solve problem (47) is then given by

$$z^{(k)} = x^{(k)} + \mu \left[H^T (y - Hx^{(k)}) - \lambda \nabla \Theta(x^{(k)}; a) \right] \quad (79a)$$

$$x^{(k+1)} = \text{soft}(z^{(k)}, \mu\lambda) \quad (79b)$$

where $0 < \mu < 2/\rho$ where ρ is the maximum eigenvalue of $H^T H$. The parameter μ can be viewed as a step-size. The soft thresholding function

$$\text{soft}(t, T) := \begin{cases} t - T, & t \geq T \\ 0, & |t| \leq T \\ t + T, & t \leq -T \end{cases} \quad (80)$$

is applied element-wise to vector $z^{(k)}$. As an FBS algorithm, it is guaranteed that $x^{(k)}$ converges to a minimizer of F .

This algorithm resembles the classical iterative shrinkage/thresholding algorithm (ISTA) [27, 33]. Note that ISTA was derived in [27, 33] using MM and was shown to converge for $0 < \mu < 1/\rho$. However, the same algorithm derived using FBS is known to converge for twice this step size. This is a practical advantage because the larger step-size generally yields faster convergence of the algorithm. We implement the algorithm with $\mu = 1.9/\rho$.

We further note that the iterative thresholding algorithm (79) has the property that $F(x^{(k)})$ monotonically decreases. For $0 < \mu < 1/\rho$, this monotonic decreasing property follows from the MM-based derivation. For $0 < \mu < 2/\rho$, the proximal theory of FBS [25, 26] ensures convergence but not the monotonic decreasing property. However, for this larger range of μ the algorithm does in fact have the monotonic decreasing property [5, 73].

7 Numerical Examples

7.1 Example 1

The 100-point sparse signal illustrated in Fig. 13(a) is convolved with the impulse response h shown in Fig. 10. The convolved signal is corrupted by additive white Gaussian noise (AWGN) with standard deviation $\sigma = 4$. The corrupted signal is shown in Fig. 13(b). To perform sparse deconvolution using BISR, we need to define

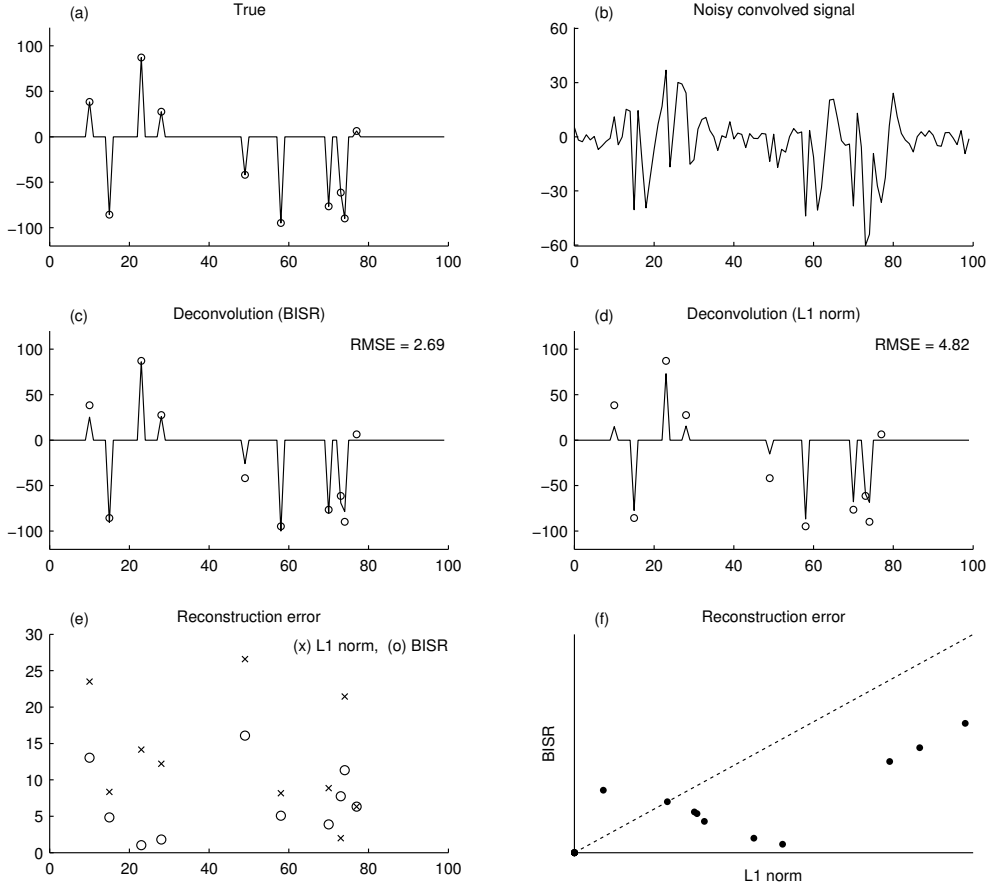


Figure 13: Example 1 of sparse deconvolution using bivariate sparse regularization (BISR).

the univariate penalty ϕ and set the regularization parameters λ and $a = (a_1, a_2)$ in the objective function (47). For ϕ , we use the arctangent penalty in Table 1. We set λ straightforwardly as

$$\lambda = \beta\sigma\|h\|_2 \quad (81)$$

which follows from an analysis of sparse optimality conditions [36, 37, 70]. We set $\beta = 2.5$, similar to the ‘three sigma’ rule. This choice of β is not intended to minimize the mean square error, but rather to inhibit false impulses appearing in the estimated sparse signal.

To set a , we use the non-negative function $P(\omega)$ shown in Fig. 10. This filter has $P(0) = 0.6$ and $P(\pi) = 0.2$. Therefore, according to Theorem 6, the objective function is convex if $0 \leq a_1 \leq 0.6/\lambda$ and $0 \leq a_2 \leq 0.2/\lambda$. To maximally induce sparsity, we set a_i to their respective maximal values. To perform deconvolution using BISR (i.e., to minimize the objective function F) we use the iterative thresholding algorithm (Sec. 6.2) with a step-size of $\mu = 1.9/\rho$. We run the algorithm until a stopping condition is satisfied. As a stopping condition, we use $\|x^{(k+1)} - x^{(k)}\|_\infty \leq 10^{-4} \times \|x^{(k)}\|_\infty$ where k is the iteration index. The run-time (averaged over 50 realizations) is about 8.8 milliseconds using a 2013 MacBook Pro (2.5 GHz Intel Core i5) running Matlab R2011a.

The BISR solution is shown in Fig. 13(c). It has a root-mean-square-error (RMSE) of 2.7, about 56% that of the ℓ_1 norm solution, shown in Fig. 13(d) for comparison. Figure 13(e) shows the reconstruction error of both solutions. The relative accuracy of the BISR solution is further illustrated in the scatter plot of Fig. 13(f), which shows the error of the two solutions plotted against each other. Most of the points lie

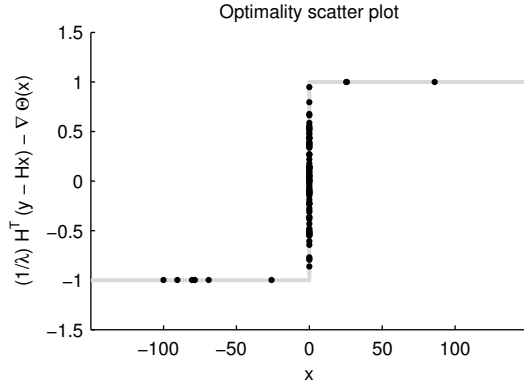


Figure 14: Optimality condition for Example 1.

Table 2: Average RMSE and run-time for Example 1

Algorithm	$\sigma=1$	$\sigma=2$	$\sigma=4$	$\sigma=8$	$\sigma=16$	(msec)
L1	1.17	2.32	4.43	8.19	13.47	3.5
L1+debiasing	0.62	1.26	2.57	5.46	11.92	3.6
Lp ($p = 0.5$)	0.66	1.19	2.39	5.12	12.05	4.3
SBR (L0)	0.65	1.15	2.38	5.33	15.35	2.1
IMSC	0.50	1.00	2.23	5.00	11.02	323.9
IPS	0.51	1.02	2.23	4.89	10.96	5.1
BISR (log)	0.52	1.11	2.53	5.62	11.58	8.2
BISR (rat)	0.51	1.06	2.41	5.42	11.46	8.6
BISR (atan)	0.50	1.03	2.30	5.13	11.22	8.8

below the diagonal line, meaning that the BISR solution has less error than the ℓ_1 norm solution.

We verify the optimality of the obtained BISR solution using (63) as illustrated by the scatter plot in Fig. 14. The obtained solution is confirmed to be a global minimizer of the objective function because the points in the scatter plot lie on the graph of the signum function.

We compare the proposed BISR method with several other algorithms in Table 2 and Fig. 15. For the comparison, we vary the noise standard deviation σ and generate 200 sparse signals and noise realizations for each value of σ . Each sparse signal consists of 10 randomly located impulses with amplitudes uniformly distributed between -100 and 100 . Table 2 gives the average RMSE and run-time (with all algorithms implemented in Matlab on the same computer).

Included in the comparison are the following methods: ℓ_1 norm regularization, ℓ_1 norm regularization with debiasing, ℓ_p pseudo-norm regularization with p of 0.5, the *single best replacement* (SBR) algorithm [74], *iterative maximally sparse convex* (IMSC) regularization [70], and the *iterative p-shrinkage* (IPS) algorithm [77, 80].

Each method provides an improvement over ℓ_1 norm regularization. The first approach is ℓ_1 norm regularization with debiasing. Debiasing is a post-processing step that applies unbiased least squares approximation to re-estimate the non-zero amplitudes [34]. This method solves the systematic underestimation of non-zero amplitudes from which ℓ_1 norm regularization suffers, but it is still influenced by noise in the observed data. As shown in Table 2, several other methods generally perform better than ℓ_1 regularization with debiasing.

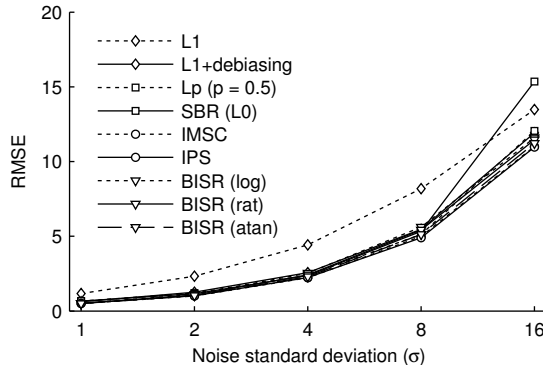


Figure 15: Average RMSE for Example 1.

Non-convex regularization using the ℓ_p pseudo-norm with $0 < p < 1$ is also a common approach for improving upon ℓ_1 norm regularization. We use $p = 0.5$ with λ set according to (81) with $\beta = 8$, a value we found worked well on average for this example. This method performed similarly as ℓ_1 norm regularization with debiasing.

For non-convex regularization using the ℓ_0 pseudo-norm we use the SBR algorithm [74]. A comparison of several methods for ℓ_0 pseudo-norm regularization showed the SBR algorithm to be state-of-the-art [70]. We use SBR with λ set according to (81) with $\beta = 70$, which we found worked well here except for high noise levels. We were unable to find a single β value that worked well over the range of σ considered here. The SBR algorithm performed similarly to ℓ_p pseudo-norm regularization, except for the highest noise level of $\sigma = 8$.

The IMSC algorithm for sparse deconvolution proceeds by solving a sequence of convex sub-problems [70]. The regularization term of each sub-problem is individually designed to be maximally non-convex (i.e., sparsity-inducing). In contrast to the proposed BISR approach, IMSC does not solve a prescribed optimization problem — each iteration yields a new convex problem to be solved. The formulation of each problem in IMSC requires the solution to a semidefinite problem (SDP); therefore, the IMSC approach is very slow. (IMSC is up to 100 times slower than other algorithms; see Table 2.) In IMSC, the parameter λ can be set the same as for ℓ_1 deconvolution; hence, we again set λ using (81) with $\beta = 2.5$. From Table 2, IMSC performs better than the preceding methods.

The IPS algorithm [77, 80] generalizes the classic iterative shrinkage-thresholding algorithm (ISTA) [27, 33]. The IPS algorithm replaces soft-thresholding in ISTA by a threshold function that does not underestimate large-amplitude signal values. Notably, IPS can be understood as a method that seeks to minimize a prescribed (albeit implicit) non-convex objective function; furthermore, each iteration of IPS can be understood as the exact minimization of a convex problem. Moreover, as IPS is an iterative thresholding algorithm, it is computationally very efficient. For this example, IPS gives excellent results when the parameter λ is set using (81) with $\beta = 2.5$. It performs about the same as IMSC but runs much faster.

To complete the comparison, we compare the proposed BISR method using the three penalties listed in Table 1. (The BISR method can be used with any penalty function satisfying the properties listed at the beginning of Sec. 2.) Referring to Table 2, the three penalties give about the same result at low noise levels; at higher noise levels, the arctangent penalty tends to perform better than the other two penalties. Compared to the other algorithms, BISR with the arctangent penalty does about as well as IPS and IMSC at low noise levels, but not quite as well at higher noise levels. Note that the proposed BISR approach is the only algorithm minimizing a prescribed convex objective function.

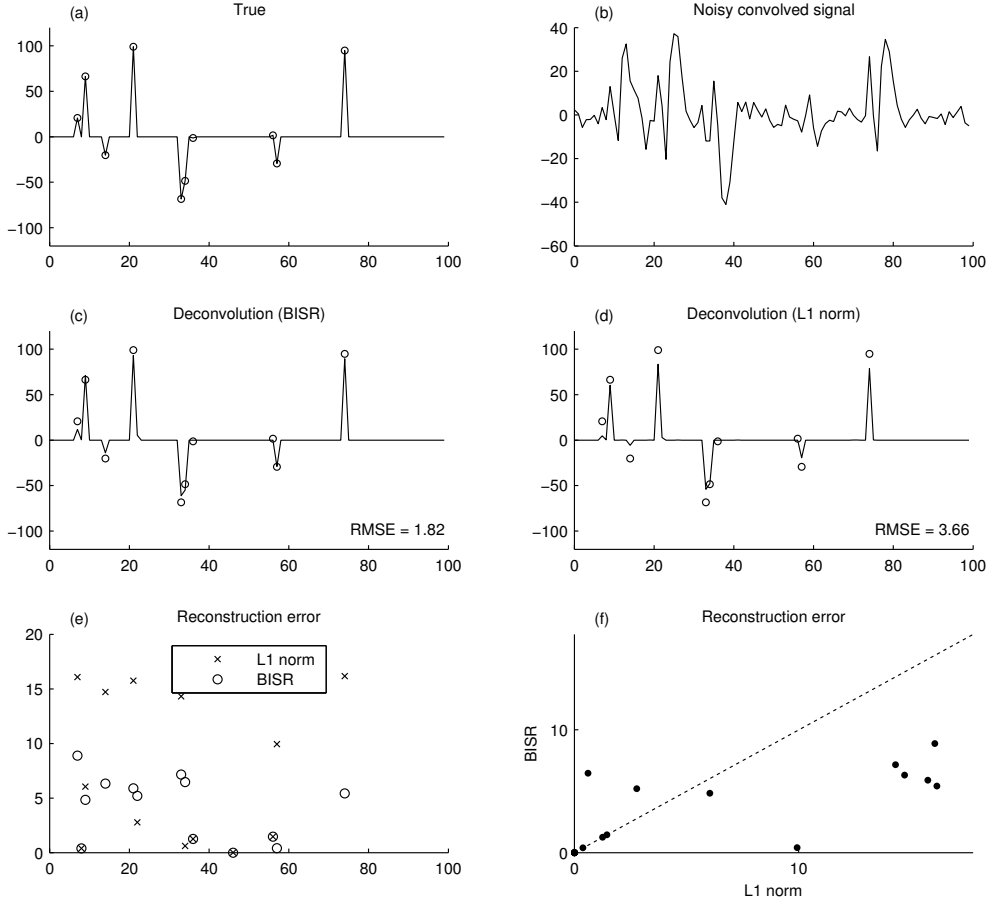


Figure 16: Example 2 of sparse deconvolution using bivariate sparse regularization (BISR).

7.2 Example 2

This is like Example 1, except we use the convolution filter H shown in Fig. 11. This filter is not invertible. The sparse signal (Fig. 16(a)) is convolved with the impulse response h and corrupted by AWGN ($\sigma = 4$). We set λ using (81) with $\beta = 2.5$ as in Example 1. Since the filter P has $P(0) = 0.76$ and $P(\pi) = 0$, Theorem 6 states that the objective function (47) is convex if $0 \leq a_1 \leq 0.76/\lambda$ and $a_2 = 0$. We run the algorithm of Sec. 6.2 with the same stopping condition to obtain the BISR solution (Fig. 16(c)). The BISR solution has an RMSE of 1.8, which is about 50% that of the ℓ_1 norm solution (Fig. 16(d)). As in Example 1, the optimality of the obtained BISR solution can be readily verified.

It is noteworthy in this example that we obtain a strictly non-convex penalty ensuring convexity of the objective function F , because in this example the convolution filter H is not invertible. It is possible only because the utilized penalty is non-separable.

In Table 3 we compare the same algorithms as in Example 1. The regularization parameter λ for each algorithm was chosen as in Example 1. The remarks made in Example 1 mostly apply here, but with a few exceptions as follows. In contrast to the generally tendency, the ℓ_p pseudo-norm performed worse than the debiased ℓ_1 norm solution for the lowest noise level ($\sigma = 1$). It appears that the performance of the ℓ_p pseudo-norm and SBR methods may degrade for low or high noise levels when one attempts to set λ proportional to σ . In addition, in contrast to Example 1, the BISR approach did not outperform ℓ_p pseudo-norm or SBR for several noise levels. IPS performs very well at most noise levels.

Table 3: Average RMSE and run-time for Example 2

Algorithm	$\sigma=1$	$\sigma=2$	$\sigma=4$	$\sigma=8$	$\sigma=16$	(msec)
L1	1.37	2.70	5.01	8.96	14.01	5.1
L1+debiasing	0.76	1.55	3.14	6.56	13.31	5.2
Lp (p = 0.5)	1.07	1.57	2.89	6.14	13.38	5.7
SBR (L0)	0.73	1.44	2.73	6.59	17.64	3.4
IMSC	0.54	1.18	2.69	6.26	12.38	305.9
IPS	0.59	1.20	2.66	5.88	12.41	6.9
BISR (log)	0.75	1.60	3.19	6.65	12.45	13.9
BISR (rat)	0.73	1.56	3.08	6.49	12.37	14.6
BISR (atan)	0.75	1.56	3.00	6.29	12.25	15.4

8 Limitations of Bivariate Penalties

The examples in Sec. 7 demonstrate the improvement attainable by non-separable bivariate penalties in comparison with separable penalties; however, the degree of improvement depends on the linear operator H in the data fidelity term. In particular, for some H , a bivariate penalty will offer little or no improvement in comparison with a separable penalty.

In reference to Figs. 10 and 11, the effectiveness of a bivariate penalty for sparse deconvolution depends on how well $|H(\omega)|^2$ can be approximated by a function $P(\omega)$ of the form (67) satisfying condition (68). Some filters H can not be well approximated by such a filter P . For example, if $H(\omega)$ is Gaussian or has a sharp peak, then it can not be well approximated by such a filter P . In this case, a bivariate penalty does not offer significant improvement in comparison with a separable penalty. For a second example, if the frequency response $H(\omega)$ has multiple nulls (e.g., a K -point moving average filter with $K > 2$), then the only filter P of the form (67) satisfying condition (68) is identically zero, $P(\omega) = 0$. In this case, the bivariate penalty reduces to the ℓ_1 norm and the proposed BISR approach offers no improvement.

In both situations, a higher-order filter P is needed to accurately approximate H , and a higher-order non-separable penalty is needed to strongly induce sparsity. Hence, to extend the applicability of non-separable sparse regularization, it will be necessary generalize the bivariate penalty to non-separable K -variate penalties ($K > 2$). Provided such an extension can be constructed, we expect the proposed BISR approach will be applicable to more general problems.

9 Conclusion

This paper aims to develop a convex approach for sparse signal estimation that improves upon ℓ_1 norm regularization, the standard convex approach. We consider ill-conditioned linear inverse problems with a quadratic data fidelity term. We focus in particular on the deconvolution problem. The proposed method is based on a non-convex penalty designed to ensure that the objective function is convex. Our previous work [70] using this idea considered only separable (additive) penalties; this is a fundamental limitation when the observation matrix is singular or near singular.

The non-separable bivariate penalty introduced in this paper overcomes this limitation. The proposed bivariate sparse regularization (BISR) approach provides a mechanism by which to improve upon ℓ_1 norm regularization while adhering to a convex framework. The greater generality of non-separable regularization, as compared with separable regularization, allows for the design of regularizers that more effectively induce

sparsity. Both BISR and ℓ_1 norm regularization lead to convex optimization problems which can be solved by similar optimization techniques.

While we have focused on deconvolution, we note that several filtering methods can be formulated as sparse deconvolution problems, e.g., peak detection [60] and denoising [69]. Hence, the proposed approach (and extensions thereof) is not limited to deconvolution.

Acknowledgment

The authors gratefully acknowledge constructive comments from the anonymous reviewers.

A Proofs

A.1 Proof of Proposition 2

Proof of Proposition 2. Let $0 \leq a \leq 1/\lambda$. By Proposition 1, s is twice continuously differentiable. Hence, so is g . Thus, to show g is convex, we show its second derivative is non-negative. From (7), we have

$$s''(t; a) \geq -a. \quad (82)$$

Since $a \leq 1/\lambda$, we have

$$s''(t; a) \geq -\frac{1}{\lambda}. \quad (83)$$

Hence

$$g''(t) = 1 + \lambda s''(t; a) \geq 0. \quad (84)$$

Therefore, g is convex. From (6), we have $f(t) = g(t) + \lambda|t|$. Since f is the sum of convex functions, f is convex. \square

A.2 Partial derivatives

Some following proofs will require the partial derivatives of $S(x; a)$. From Definition 2, they are as follows.

$$\frac{\partial S}{\partial x_1}(x; a) = \begin{cases} s'(x_1 + rx_2; \alpha), & x \in A_1 \\ rs'(rx_1 + x_2; \alpha) + (1-r)s'(x_1; a_1), & x \in A_2 \\ rs'(rx_1 + x_2; \alpha) + (1+r)s'(x_1; a_2), & x \in A_3 \\ s'(x_1 + rx_2; \alpha), & x \in A_4 \end{cases} \quad (85)$$

$$\frac{\partial S}{\partial x_2}(x; a) = \begin{cases} rs'(x_1 + rx_2; \alpha) + (1-r)s'(x_2; a_1), & x \in A_1 \\ s'(rx_1 + x_2; \alpha), & x \in A_2 \\ s'(rx_1 + x_2; \alpha), & x \in A_3 \\ rs'(x_1 + rx_2; \alpha) + (1+r)s'(x_2; a_2), & x \in A_4 \end{cases} \quad (86)$$

$$\frac{\partial^2 S}{\partial^2 x_1}(x; a) = \begin{cases} s''(x_1 + rx_2; \alpha), & x \in A_1 \\ r^2 s''(rx_1 + x_2; \alpha) + (1-r)s''(x_1; a_1), & x \in A_2 \\ r^2 s''(rx_1 + x_2; \alpha) + (1+r)s''(x_1; a_2), & x \in A_3 \\ s''(x_1 + rx_2; \alpha), & x \in A_4 \end{cases} \quad (87)$$

$$\frac{\partial^2 S}{\partial^2 x_2}(x; a) = \begin{cases} r^2 s''(x_1 + rx_2; \alpha) + (1 - r) s''(x_2; a_1), & x \in A_1 \\ s''(rx_1 + x_2; \alpha), & x \in A_2 \\ s''(rx_1 + x_2; \alpha), & x \in A_3 \\ r^2 s''(x_1 + rx_2; \alpha) + (1 + r) s''(x_2; a_2), & x \in A_4 \end{cases} \quad (88)$$

$$\frac{\partial^2 S}{\partial x_1 \partial x_2}(x; a) = \begin{cases} r s''(x_1 + rx_2; \alpha), & x \in A_1 \\ r s''(rx_1 + x_2; \alpha), & x \in A_2 \\ r s''(rx_1 + x_2; \alpha), & x \in A_3 \\ r s''(x_1 + rx_2; \alpha), & x \in A_4 \end{cases} \quad (89)$$

A.3 Scaling identities

Some following proofs will use scaling identities. From the scaling property in Sec. 2, it follows that

$$s(t, \alpha) = \frac{a_1}{\alpha} s\left(\frac{\alpha}{a_1} t; a_1\right) \quad (90)$$

$$= (1 + r) s\left(\frac{t}{1 + r}; a_1\right) \quad (91)$$

and similarly

$$s(t, a_1) = \frac{1}{1 + r} s((1 + r)t; \alpha) \quad (92)$$

$$s'(t, a_1) = s'((1 + r)t; \alpha) \quad (93)$$

$$s''(t, a_1) = (1 + r) s''((1 + r)t; \alpha). \quad (94)$$

Likewise,

$$s(t, \alpha) = \frac{a_2}{\alpha} s\left(\frac{\alpha}{a_2} t; a_2\right) \quad (95)$$

$$= (1 - r) s\left(\frac{t}{1 - r}; a_2\right) \quad (96)$$

and

$$s(t, a_2) = \frac{1}{1 - r} s((1 - r)t; \alpha) \quad (97)$$

$$s'(t, a_2) = s'((1 - r)t; \alpha) \quad (98)$$

$$s''(t, a_2) = (1 - r) s''((1 - r)t; \alpha). \quad (99)$$

A.4 Proof of Lemma 1

Proof of Lemma 1. We first show that S in Definition 2 is consistent on the common boundaries of the sets A_i . Consider the common boundary of A_1 and A_4 , i.e., the line $\{(x_1, 0) : x_1 \in \mathbb{R}\}$. From the A_1 side,

$$S(x; a) \Big|_{\substack{x_2=0 \\ x \in A_1}} = s(x_1; \alpha) + (1 - r) s(0; a_1) \quad (100)$$

$$= s(x_1; \alpha) \quad (101)$$

where we used $s(0; \cdot) = 0$. From the A_4 side,

$$S(x; a) \Big|_{\substack{x_2=0 \\ x \in A_4}} = s(x_1; \alpha) + (1+r)s(0; a_2) \quad (102)$$

$$= s(x_1; \alpha). \quad (103)$$

Hence, S is consistently defined on the common boundary of A_1 and A_4 .

Consider the common boundary of A_1 and A_2 , i.e., the line $\{(x_1, x_1) : x_1 \in \mathbb{R}\}$. From the A_1 side,

$$S(x; a) \Big|_{\substack{x_2=x_1 \\ x \in A_1}} = s((1+r)x_1; \alpha) + (1-r)s(x_1; a_1). \quad (104)$$

From the A_2 side,

$$S(x; a) \Big|_{\substack{x_2=x_1 \\ x \in A_2}} = s((1+r)x_1; \alpha) + (1-r)s(x_1; a_2). \quad (105)$$

Hence, S is consistently defined on the common boundary of A_1 and A_2 . Similarly, it can be shown that S is consistently defined on the other common boundaries of the sets A_i . Hence S is continuous because s is continuous.

We now show S is differentiable on \mathbb{R}^2 . We need only show S is differentiable on the common boundaries of the sets A_i because s is differentiable. Consider the common boundary of A_1 and A_4 . From the A_1 side,

$$\frac{\partial S}{\partial x_1}(x; a) \Big|_{\substack{x_2 \rightarrow 0 \\ x \in A_1}} = s'(x_1; \alpha) \quad (106)$$

using (85), and

$$\frac{\partial S}{\partial x_2}(x; a) \Big|_{\substack{x_2 \rightarrow 0 \\ x \in A_1}} = rs'(x_1; \alpha) + (1-r)s'(0; a_1) \quad (107)$$

$$= rs'(x_1; \alpha) \quad (108)$$

using (86) and $s'(0, \cdot) = 0$. From the A_4 side,

$$\frac{\partial S}{\partial x_1}(x; a) \Big|_{\substack{x_2 \rightarrow 0 \\ x \in A_4}} = s'(x_1; \alpha) \quad (109)$$

and

$$\frac{\partial S}{\partial x_2}(x; a) \Big|_{\substack{x_2 \rightarrow 0 \\ x \in A_4}} = rs'(x_1; \alpha) + (1+r)s'(0; a_2) \quad (110)$$

$$= rs'(x_1; \alpha). \quad (111)$$

Hence, the partial derivatives of S are continuous on the common of boundary of A_1 and A_4 .

Consider the common boundary of A_1 and A_2 . From the A_1 side,

$$\frac{\partial S}{\partial x_1}(x; a) \Big|_{\substack{x_2 \rightarrow x_1 \\ x \in A_1}} = s'((1+r)x_1; \alpha) \quad (112)$$

$$= s'(x_1; a_1) \quad (113)$$

where we used the scaling property (11) and identity (21). Also, using the same properties,

$$\frac{\partial S}{\partial x_2}(x; a) \Big|_{\substack{x_2 \rightarrow x_1 \\ x \in A_1}} = rs'((1+r)x_1; \alpha) + (1-r)s'(x_1; a_1) \quad (114)$$

$$= s'(x_1; a_1). \quad (115)$$

From the A_2 side, we similarly have

$$\frac{\partial S}{\partial x_1}(x; a) \Big|_{\substack{x_2 \rightarrow x_1 \\ x \in A_2}} = rs'((1+r)x_1; \alpha) + (1-r)s'(x_1; a_1) \quad (116)$$

$$= s'(x_1; a_1) \quad (117)$$

and

$$\frac{\partial S}{\partial x_2}(x; a) \Big|_{\substack{x_2 \rightarrow x_1 \\ x \in A_2}} = s'((1+r)x_1; \alpha). \quad (118)$$

$$= s'(x_1; a_1). \quad (119)$$

Hence, the partial derivatives of S are continuous on the common of boundary of A_1 and A_2 . Similarly, it can be shown that the partial derivatives of S are continuous on the other common boundaries of the sets A_i . Hence S is differentiable on \mathbb{R}^2 .

We now show S is twice differentiable. We need only show the second-order partial derivatives of S are continuous on the common boundaries of the sets A_i because s is twice differentiable.

Consider the common boundary of A_1 and A_4 . Using (87), we obtain

$$\frac{\partial^2 S}{\partial^2 x_1}(x; a) \Big|_{\substack{x_2 \rightarrow 0 \\ x \in A_1}} = s''(x_1; \alpha) \quad (120)$$

and

$$\frac{\partial^2 S}{\partial^2 x_1}(x; a) \Big|_{\substack{x_2 \rightarrow 0 \\ x \in A_4}} = s''(x_1; \alpha). \quad (121)$$

Hence $\partial^2 S / \partial^2 x_1$ is continuous on the common boundary of A_1 and A_4 . Using (88), we obtain

$$\frac{\partial^2 S}{\partial^2 x_2}(x; a) \Big|_{\substack{x_2 \rightarrow 0 \\ x \in A_1}} = r^2 s''(x_1; \alpha) + (1-r)s''(0; a_1) \quad (122)$$

$$= r^2 s''(x_1; \alpha) - (1-r)a_1 \quad (123)$$

where we used $s''(0; a_1) = -a_1$, and

$$\frac{\partial^2 S}{\partial^2 x_2}(x; a) \Big|_{\substack{x_2 \rightarrow 0 \\ x \in A_4}} = r^2 s''(x_1; \alpha) + (1+r)s''(0; a_2) \quad (124)$$

$$= r^2 s''(x_1; \alpha) - (1+r)a_2 \quad (125)$$

where we used $s''(0; a_2) = -a_2$. Using (15), we have

$$(1-r)a_1 = (1+r)a_2 = \frac{2a_1 a_2}{a_1 + a_2}, \quad (126)$$

hence $\partial^2 S / \partial^2 x_2$ is continuous on the common boundary of A_1 and A_4 .

Consider the common boundary of A_1 and A_2 . Using (87), we obtain

$$\frac{\partial^2 S}{\partial^2 x_1}(x; a) \Big|_{\substack{x_2 \rightarrow x_1 \\ x \in A_1}} = s''((1+r)x_1; \alpha) \quad (127)$$

and

$$\frac{\partial^2 S}{\partial^2 x_1}(x; a) \Big|_{\substack{x_2 \rightarrow x_1 \\ x \in A_2}} = r^2 s''((1+r)x_1; \alpha) + (1-r)s''(x_1; a_1) \quad (128)$$

$$= r^2 s''((1+r)x_1; \alpha) + (1-r)(1+r)s''((1+r)x_1; \alpha) \quad (129)$$

$$= s''((1+r)x_1; \alpha) \quad (130)$$

where we used (94). Hence $\partial^2 S / \partial^2 x_2$ is continuous on the common boundary of A_1 and A_2 .

Similarly, it can be shown that the remaining partial derivatives are continuous on the other common boundaries of the sets A_i . Hence S is twice continuously differentiable on \mathbb{R}^2 .

We now show S is concave by showing that $\nabla^2 S(x)$ is negative semidefinite for all $x \in \mathbb{R}^2$. Specifically, we show that $-\nabla^2 S(x)$ is positive semidefinite by showing that its principal minors are non-negative (Sylvester's criterion).

The determinant of the Hessian of S

$$\det[\nabla^2 S(x)] = \frac{\partial^2 S}{\partial^2 x_1} \frac{\partial^2 S}{\partial^2 x_2} - \left(\frac{\partial^2 S}{\partial x_1 \partial x_2} \right)^2 \quad (131)$$

is given by

$$\det[\nabla^2 S(x; a)] = \quad (132)$$

$$\begin{cases} (1-r) s''(x_2; a_1) s''(x_1 + rx_2; \alpha), & x \in A_1 \\ (1-r) s''(x_1; a_1) s''(rx_1 + x_2; \alpha), & x \in A_2 \\ (1+r) s''(x_1; a_2) s''(rx_1 + x_2; \alpha), & x \in A_3 \\ (1+r) s''(x_2; a_2) s''(x_1 + rx_2; \alpha), & x \in A_4. \end{cases}$$

Since $s''(t; \cdot)$ is negative for all t and $|r|$ is bounded by 1, it follows that $\det[\nabla^2 S(x)]$ is non-negative for all $x \in \mathbb{R}^2$. Hence, the determinant of $-\nabla^2 S(x)$ is non-negative. Moreover, $\partial^2 S / \partial^2 x_i(x; a) \leq 0$ for all $x \in \mathbb{R}^2$ for $i = 1, 2$. Hence, the principal minors of $-\nabla^2 S(x)$ are non-negative. This proves S is concave on \mathbb{R}^2 . \square

A.5 Proof of Lemma 2

Using (87)-(89), the Hessian of S is given by

$$\nabla^2 S(x; a) = \begin{cases} \begin{bmatrix} s''(x_1 + rx_2; \alpha) & rs''(x_1 + rx_2; \alpha) \\ rs''(x_1 + rx_2; \alpha) & r^2 s''(x_1 + rx_2; \alpha) + (1-r) s''(x_2; a_1) \end{bmatrix}, & x \in A_1 \\ \begin{bmatrix} r^2 s''(rx_1 + x_2; \alpha) + (1-r) s''(x_1; a_1) & rs''(rx_1 + x_2; \alpha) \\ rs''(rx_1 + x_2; \alpha) & s''(rx_1 + x_2; \alpha) \end{bmatrix}, & x \in A_2 \\ \begin{bmatrix} r^2 s''(rx_1 + x_2; \alpha) + (1+r) s''(x_1; a_2) & rs''(rx_1 + x_2; \alpha) \\ rs''(rx_1 + x_2; \alpha) & s''(rx_1 + x_2; \alpha) \end{bmatrix}, & x \in A_3 \\ \begin{bmatrix} s''(x_1 + rx_2; \alpha) & rs''(x_1 + rx_2; \alpha) \\ rs''(x_1 + rx_2; \alpha) & r^2 s''(x_1 + rx_2; \alpha) + (1+r) s''(x_2; a_2) \end{bmatrix}, & x \in A_4. \end{cases} \quad (133)$$

We write this as

$$\nabla^2 S(x; a) = \begin{cases} s''(x_1 + rx_2; \alpha) \begin{bmatrix} 1 & r \\ r & r^2 \end{bmatrix} + s''(x_2; a_1) \begin{bmatrix} 0 & 0 \\ 0 & 1-r \end{bmatrix}, & x \in A_1 \\ s''(rx_1 + x_2; \alpha) \begin{bmatrix} r^2 & r \\ r & 1 \end{bmatrix} + s''(x_1; a_1) \begin{bmatrix} 1-r & 0 \\ 0 & 0 \end{bmatrix}, & x \in A_2 \\ s''(rx_1 + x_2; \alpha) \begin{bmatrix} r^2 & r \\ r & 1 \end{bmatrix} + s''(x_1; a_2) \begin{bmatrix} 1+r & 0 \\ 0 & 0 \end{bmatrix}, & x \in A_3 \\ s''(x_1 + rx_2; \alpha) \begin{bmatrix} 1 & r \\ r & r^2 \end{bmatrix} + s''(x_2; a_2) \begin{bmatrix} 0 & 0 \\ 0 & 1+r \end{bmatrix}, & x \in A_4. \end{cases} \quad (134)$$

Using (94) and (99), we write (134) as

$$\nabla^2 S(x; a) = \begin{cases} s''(x_1 + rx_2; \alpha) \begin{bmatrix} 1 & r \\ r & r^2 \end{bmatrix} + s''((1+r)x_2; \alpha) \begin{bmatrix} 0 & 0 \\ 0 & 1-r^2 \end{bmatrix}, & x \in A_1 \\ s''(rx_1 + x_2; \alpha) \begin{bmatrix} r^2 & r \\ r & 1 \end{bmatrix} + s''((1+r)x_1; \alpha) \begin{bmatrix} 1-r^2 & 0 \\ 0 & 0 \end{bmatrix}, & x \in A_2 \\ s''(rx_1 + x_2; \alpha) \begin{bmatrix} r^2 & r \\ r & 1 \end{bmatrix} + s''((1-r)x_1; \alpha) \begin{bmatrix} 1-r^2 & 0 \\ 0 & 0 \end{bmatrix}, & x \in A_3 \\ s''(x_1 + rx_2; \alpha) \begin{bmatrix} 1 & r \\ r & r^2 \end{bmatrix} + s''((1-r)x_2; \alpha) \begin{bmatrix} 0 & 0 \\ 0 & 1-r^2 \end{bmatrix}, & x \in A_4. \end{cases} \quad (135)$$

Proof of Theorem 2. Note that the matrices in (135) are positive semidefinite because $|r| \leq 1$. We also have $-\alpha \leq s''(t; \alpha) < 0$ for all t . Hence,

$$\nabla^2 S(x; a) \succcurlyeq -\alpha \begin{bmatrix} 1 & r \\ r & 1 \end{bmatrix}, \quad x \in \mathbb{R}^2. \quad (136)$$

Using (15) and (22), we write (136) as

$$\nabla^2 S(x; a) \succcurlyeq -\frac{1}{2} \begin{bmatrix} a_1 + a_2 & a_1 - a_2 \\ a_1 - a_2 & a_1 + a_2 \end{bmatrix}. \quad (137)$$

Since $s''(0; \alpha) = -\alpha$ [see (8)], we similarly have

$$\nabla^2 S(0; a) = -\frac{1}{2} \begin{bmatrix} a_1 + a_2 & a_1 - a_2 \\ a_1 - a_2 & a_1 + a_2 \end{bmatrix}. \quad (138)$$

□

A.6 Proof of Theorem 3

Proof of Theorem 3. Without loss of generality, assume $a_1 > a_2$. From (32) and (6), the inequality (36) can be written as

$$s(x_1; a_1) + s(x_2; a_1) \leq S(x; a) \leq s(x_1; a_2) + s(x_2; a_2) \quad (139)$$

where S is given in Definition 2. First we prove (139) for $x \in A_1$. Second, we prove it for $x \in A_3$. The proofs for $x \in A_2$ and $x \in A_4$ are essentially identical by symmetries. Note that since $a_1 \geq a_2 \geq 0$, we have $a_1 \geq \alpha \geq a_2$ and $0 \leq r \leq 1$.

Let $x \in A_1$. We seek to prove

$$s(x_1 + rx_2; \alpha) + (1 - r) s(x_2; a_1) \geq s(x_1; a_1) + s(x_2; a_1). \quad (140)$$

Using (91), we have

$$s(x_1 + rx_2; \alpha) = (1 + r) s\left(\frac{x_1 + rx_2}{1 + r}; a_1\right) \quad (141)$$

$$\geq (1 + r) \left[\frac{1}{1 + r} s(x_1; a_1) + \frac{r}{1 + r} s(x_2; a_1) \right] \quad (142)$$

$$= s(x_1; a_1) + r s(x_2; a_1) \quad (143)$$

where the inequality is due to s being a concave function. Adding $(1 - r) s(x_2; a_1)$ to both sides of (143) gives (140).

Let $x \in A_1$. (That is, $0 \leq x_2 \leq x_1$ or $x_1 \leq x_2 \leq 0$.) We seek to prove

$$s(x_1; a_2) + s(x_2; a_2) \geq s(x_1 + rx_2; \alpha) + (1 - r) s(x_2; a_1). \quad (144)$$

From (91) we have

$$s(x_2; a_1) = \frac{1}{1 + r} s((1 + r)x_2; \alpha). \quad (145)$$

Suppose $0 \leq x_2 \leq x_1$. As s is concave and $s(0; \cdot) = 0$, we have

$$s(x_1; \alpha) \geq \frac{x_1}{x_1 + rx_2} s(x_1 + rx_2; \alpha) \quad (146)$$

because $0 \leq x_1 \leq x_1 + rx_2$. Similarly,

$$s((1 + r)x_2; \alpha) \geq \frac{(1 + r)x_2}{x_1 + rx_2} s(x_1 + rx_2; \alpha) \quad (147)$$

because $0 \leq (1 + r)x_2 \leq x_1 + rx_2$. From (145) and (147) it follows that

$$rs(x_2; a_1) \geq \frac{rx_2}{x_1 + rx_2} s(x_1 + rx_2; \alpha). \quad (148)$$

Adding (146) and (148) gives

$$s(x_1; \alpha) + rs(x_2; a_1) \geq s(x_1 + rx_2; \alpha). \quad (149)$$

Adding $(1 - r) s(x_2; a_1)$ to both sides of (149) gives

$$s(x_1; \alpha) + s(x_2; a_1) \geq s(x_1 + rx_2; \alpha) + (1 - r) s(x_2; a_1). \quad (150)$$

Since $\alpha \geq a_2$, we have $s(x_1; a_2) \geq s(x_1; \alpha)$. Similarly, since $a_1 \geq a_2$, we have $s(x_2; a_2) \geq s(x_2; a_1)$. It follows that (144) holds. For $x_1 \leq x_2 \leq 0$ the proof is similar.

Let $x \in A_3$. We seek to prove

$$s(rx_1 + x_2; \alpha) + (1 + r) s(x_1; a_2) \geq s(x_1; a_1) + s(x_2; a_1). \quad (151)$$

Suppose $x_2 \geq -x_1 \geq 0$. Since $0 \leq r \leq 1$ it follows that $0 \leq rx_1 + x_2 \leq x_2$. As s is concave and $s(0; \cdot) = 0$, we have

$$s(rx_1 + x_2; \alpha) \geq \frac{rx_1 + x_2}{x_2} s(x_2; \alpha) \quad (152)$$

and

$$s(x_1; \alpha) = s(-x_1; \alpha) \geq -\frac{x_1}{x_2} s(x_2; \alpha) \quad (153)$$

where we use the fact that s is symmetric. Multiplying (153) by r and adding (152), we have

$$s(rx_1 + x_2; \alpha) + rs(x_1; \alpha) \geq s(x_2; \alpha) \quad (154)$$

Since $a_2 \leq \alpha$, we have $s(x_1; a_2) \geq s(x_1; \alpha)$. Multiplying by $(1+r)$ and rearranging, we have

$$(1+r)s(x_1; a_2) - rs(x_1; \alpha) \geq s(x_1; \alpha). \quad (155)$$

Adding (154) and (155), we have

$$s(rx_1 + x_2; \alpha) + (1+r)s(x_1; a_2) \geq s(x_1; \alpha) + s(x_2; \alpha). \quad (156)$$

Since $\alpha \leq a_1$, we have $s(t; \alpha) \geq s(t; a_1)$ for all t . It follows that (151) holds. For $x_2 \leq -x_1 \leq 0$ the proof is similar.

Let $x \in A_3$. We seek to prove

$$s(rx_1 + x_2; \alpha) + (1+r)s(x_1; a_2) \leq s(x_1; a_2) + s(x_2; a_2). \quad (157)$$

From (96) we have

$$s(rx_1 + x_2; \alpha) = (1-r)s\left(\frac{rx_1 + x_2}{1-r}; a_2\right). \quad (158)$$

Since s is symmetric, we have $s(x_1; a_2) = s(-x_1; a_2)$. Hence

$$s(rx_1 + x_2; \alpha) + rs(x_1; a_2) = (1-r)s\left(\frac{rx_1 + x_2}{1-r}; a_2\right) + rs(-x_1; a_2) \quad (159)$$

$$\leq s\left((1-r)\frac{rx_1 + x_2}{1-r} - rx_1; a_2\right) \quad (160)$$

$$= s(x_2; a_2) \quad (161)$$

where the inequality is due to s being a concave function. Adding $s(x_1; a_2)$ to both sides of (161) gives the desired inequality (157). \square

A.7 Proof of Lemma 4

Proof of Lemma 4. We express F in (47) as

$$F(x) = \frac{1}{2}\|y - Hx\|_2^2 + \frac{\lambda}{2} \sum_n \psi((x_{n-1}, x_n); a) \quad (162)$$

$$= \frac{1}{2}y^\top y - y^\top Hx + \frac{1}{2}x^\top (H^\top H - P)x + g(x) \quad (163)$$

where $g: \mathbb{R}^N \rightarrow \mathbb{R}$ is defined as

$$g(x) = \frac{1}{2}x^\top Px + \frac{\lambda}{2} \sum_n \psi((x_{n-1}, x_n); a). \quad (164)$$

The first three terms are convex. Hence F is convex if g is convex. We express P as a sum of matrices, each comprising a single 2×2 block.

$$P = \cdots + \begin{bmatrix} 0 & & & \\ & \frac{1}{2}p_0 & p_1 & \\ & p_1 & \frac{1}{2}p_0 & \\ & & & 0 \end{bmatrix} + \begin{bmatrix} 0 & & & \\ & 0 & & \\ & & \frac{1}{2}p_0 & p_1 \\ & & p_1 & \frac{1}{2}p_0 \\ & & & & 0 \end{bmatrix} + \cdots \quad (165)$$

Hence g may be expressed as

$$g(x) = \frac{1}{2} \sum_n \left((x_{n-1}, x_n) \begin{bmatrix} \frac{1}{2}p_0 & p_1 \\ p_1 & \frac{1}{2}p_0 \end{bmatrix} \begin{pmatrix} x_{n-1} \\ x_n \end{pmatrix} + \lambda\psi((x_{n-1}, x_n); a) \right) \quad (166)$$

$$= \frac{1}{2} \sum_n f((x_{n-1}, x_n)) \quad (167)$$

where $f: \mathbb{R}^2 \rightarrow \mathbb{R}$ is given by (49). If f is convex, then g is the sum of convex functions and is thus convex itself. \square

References

- [1] A. Achim and E. E. Kuruoğlu. Image denoising using bivariate α -stable distributions in the complex wavelet domain. *IEEE Signal Processing Letters*, 12(1):17–20, January 2005.
- [2] M. V. Afonso, J. M. Bioucas-Dias, and M. A. T. Figueiredo. Fast image recovery using variable splitting and constrained optimization. *IEEE Trans. Image Process.*, 19(9):2345–2356, September 2010.
- [3] M. S. Asif and J. Romberg. Fast and accurate algorithms for re-weighted l_1 -norm minimization. *IEEE Trans. Signal Process.*, 61(23):5905–5916, December 2013.
- [4] F. Bach, R. Jenatton, J. Mairal, and G. Obozinski. Optimization with sparsity-inducing penalties. *Foundations and Trends in Machine Learning*, 4(1):1–106, 2012.
- [5] İ. Bayram. On the convergence of the iterative shrinkage/thresholding algorithm with a weakly convex penalty. <http://arxiv.org/abs/1510.07821>, October 2015.
- [6] İ. Bayram. Penalty functions derived from monotone mappings. *IEEE Signal Processing Letters*, 22(3):265–269, March 2015.
- [7] I. Bayram, P.-Y. Chen, and I. Selesnick. Fused lasso with a non-convex sparsity inducing penalty. In *Proc. IEEE Int. Conf. Acoust., Speech, Signal Processing (ICASSP)*, May 2014.
- [8] A. Beck and M. Teboulle. A fast iterative shrinkage-thresholding algorithm for linear inverse problems. *SIAM J. Imag. Sci.*, 2(1):183–202, 2009.
- [9] A. Blake and A. Zisserman. *Visual Reconstruction*. MIT Press, 1987.
- [10] A. Blumensath. Accelerated iterative hard thresholding. *Signal Processing*, 92(3):752–756, 2012.
- [11] S. Boyd and L. Vandenberghe. *Convex Optimization*. Cambridge University Press, 2004.
- [12] A. Bruckstein, D. Donoho, and M. Elad. From sparse solutions of systems of equations to sparse modeling of signals and images. *SIAM Review*, 51(1):34–81, 2009.

- [13] C. L. Byrne. *Iterative Optimization in Inverse Problems*. CRC Press, 2014.
- [14] E. J. Candès, M. B. Wakin, and S. Boyd. Enhancing sparsity by reweighted l1 minimization. *J. Fourier Anal. Appl.*, 14(5):877–905, December 2008.
- [15] P. Charbonnier, L. Blanc-Feraud, G. Aubert, and M. Barlaud. Deterministic edge-preserving regularization in computed imaging. *IEEE Trans. Image Process.*, 6(2):298–311, February 1997.
- [16] R. Chartrand. Fast algorithms for nonconvex compressive sensing: MRI reconstruction from very few data. In *IEEE Int. Symp. Biomed. Imag. (ISBI)*, pages 262–265, July 2009.
- [17] R. Chartrand. Nonconvex splitting for regularized low-rank + sparse decomposition. *IEEE Trans. Signal Process.*, 60(11):5810–5819, November 2012.
- [18] R. Chartrand. Shrinkage mappings and their induced penalty functions. In *Proc. IEEE Int. Conf. Acoust., Speech, Signal Processing (ICASSP)*, pages 1026–1029, May 2014.
- [19] R. Chartrand, E. Y. Sidky, and P. Xiaochuan. Nonconvex compressive sensing for X-ray CT: an algorithm comparison. In *Asilomar Conf. on Signals, Systems and Computers*, pages 665–669, November 2013.
- [20] L. Chen and Y. Gu. The convergence guarantees of a non-convex approach for sparse recovery. *IEEE Trans. Signal Process.*, 62(15):3754–3767, August 2014.
- [21] P.-Y. Chen and I. W. Selesnick. Group-sparse signal denoising: Non-convex regularization, convex optimization. *IEEE Trans. Signal Process.*, 62(13):3464–3478, July 2014.
- [22] H. Chipman, E. Kolaczyk, and R. McCulloch. Adaptive Bayesian wavelet shrinkage. *J. Am. Stat. Assoc.*, 92(440):1413–1421, December 1997.
- [23] E. Chouzenoux, A. Jezierska, J. Pesquet, and H. Talbot. A majorize-minimize subspace approach for $\ell_2 - \ell_0$ image regularization. *SIAM J. Imag. Sci.*, 6(1):563–591, 2013.
- [24] P. L. Combettes and J.-C. Pesquet. Proximal thresholding algorithm for minimization over orthonormal bases. *SIAM J. Optim.*, 18(4):1351–1376, 2008.
- [25] P. L. Combettes and J.-C. Pesquet. Proximal splitting methods in signal processing. In H. H. Bauschke et al., editors, *Fixed-Point Algorithms for Inverse Problems in Science and Engineering*, pages 185–212. Springer-Verlag, 2011.
- [26] P. L. Combettes and V. R. Wajs. Signal recovery by proximal forward-backward splitting. *Multiscale Modeling & Simulation*, 4(4):1168–1200, 2005.
- [27] I. Daubechies, M. Defriese, and C. De Mol. An iterative thresholding algorithm for linear inverse problems with a sparsity constraint. *Commun. Pure Appl. Math.*, LVII:1413–1457, 2004.
- [28] I. Daubechies, R. DeVore, M. Fornasier, and C. Gunturk. Iteratively reweighted least squares minimization for sparse recovery. *Comm. Pure App. Math.*, 63(1):1–38, January 2010.
- [29] Y. Ding and I. W. Selesnick. Artifact-free wavelet denoising: Non-convex sparse regularization, convex optimization. *IEEE Signal Processing Letters*, 22(9):1364–1368, September 2015.
- [30] B. Dumitrescu. *Positive trigonometric polynomials and signal processing applications*. Springer, 2007.

- [31] J. M. Fadili and L. Boubchir. Analytical form for a Bayesian wavelet estimator of images using the Bessel K form densities. *IEEE Trans. Image Process.*, 14(2):231–240, February 2005.
- [32] M. Figueiredo, J. Bioucas-Dias, and R. Nowak. Majorization-minimization algorithms for wavelet-based image restoration. *IEEE Trans. Image Process.*, 16(12):2980–2991, December 2007.
- [33] M. Figueiredo and R. Nowak. An EM algorithm for wavelet-based image restoration. *IEEE Trans. Image Process.*, 12(8):906–916, August 2003.
- [34] M. A. T. Figueiredo, R. D. Nowak, and S. J. Wright. Gradient projection for sparse reconstruction: Application to compressed sensing and other inverse problems. *IEEE J. Sel. Top. Signal Process.*, 1(4):586–598, December 2007.
- [35] S. Foucart. Hard thresholding pursuit: an algorithm for compressive sensing. *SIAM J. Numer. Anal.*, 49(6):2543–2563, 2010.
- [36] J.-J. Fuchs. Convergence of a sparse representations algorithm applicable to real or complex data. *IEEE J. Sel. Top. Signal Processing*, 1(4):598–605, December 2007.
- [37] J. J. Fuchs. Identification of real sinusoids in noise, the global matched filter approach. In *15th IFAC Symp. on System Identification*, pages 1127–1132, Saint-Malo, France, July 2009.
- [38] G. Gasso, A. Rakotomamonjy, and S. Canu. Recovering sparse signals with a certain family of nonconvex penalties and DC programming. *IEEE Trans. Signal Process.*, 57(12):4686–4698, December 2009.
- [39] D. Geman and G. Reynolds. Constrained restoration and the recovery of discontinuities. *IEEE Trans. Pattern Anal. and Machine Intel.*, 14(3):367–383, March 1992.
- [40] A. Gholami and S. M. Hosseini. A general framework for sparsity-based denoising and inversion. *IEEE Trans. Signal Process.*, 59(11):5202–5211, November 2011.
- [41] T. Goldstein and S. Osher. The split Bregman method for L1-regularized problems. *SIAM J. Imag. Sci.*, 2(2):323–343, 2009.
- [42] G. Harikumar and Y. Bresler. A new algorithm for computing sparse solutions to linear inverse problems. In *Proc. IEEE Int. Conf. Acoust., Speech, Signal Processing (ICASSP)*, volume 3, pages 1331–1334, May 1996.
- [43] M. W. Jacobson and J. A. Fessler. An expanded theoretical treatment of iteration-dependent majorize-minimize algorithms. *IEEE Trans. Image Process.*, 16(10):2411–2422, October 2007.
- [44] N. Kingsbury and T. Reeves. Redundant representation with complex wavelets: how to achieve sparsity. In *Proc. IEEE Int. Conf. Image Processing (ICIP)*, volume 1, pages 45–48, 2003.
- [45] I. Kozlov and A. Petukhov. Sparse solutions of underdetermined linear systems. In W. Freeden et al., editor, *Handbook of Geomathematics*. Springer, 2010.
- [46] K. Lange, E. C. Chi, and H. Zhou. A brief survey of modern optimization for statisticians. *Int. Stat. Rev.*, 82(1):46–70, 2014.
- [47] A. Lanza, S. Morigi, and F. Sgallari. Convex image denoising via non-convex regularization. In J.-F. Aujol, M. Nikolova, and N. Papadakis, editors, *Scale Space and Variational Methods in Computer Vision*, volume 9087 of *Lecture Notes in Computer Science*, pages 666–677. Springer, 2015.

- [48] P.-L. Loh and M. J. Wainwright. Regularized M-estimators with nonconvexity: Statistical and algorithmic theory for local optima. *J. Machine Learning Research*, 16:559–616, 2015.
- [49] D. A. Lorenz. Non-convex variational denoising of images: Interpolation between hard and soft wavelet shrinkage. *Current Development in Theory and Application of Wavelets*, 1(1):31–56, 2007.
- [50] D. Malioutov and A. Aravkin. Iterative log thresholding. In *Proc. IEEE Int. Conf. Acoust., Speech, Signal Processing (ICASSP)*, pages 7198–7202, May 2014.
- [51] S. Mallat. *A wavelet tour of signal processing*. Academic Press, 1998.
- [52] Y. Marnissi, A. Benazza-Benyahia, E. Chouzenoux, and J.-C. Pesquet. Generalized multivariate exponential power prior for wavelet-based multichannel image restoration. In *Proc. IEEE Int. Conf. Image Processing (ICIP)*, pages 2402–2406, September 2013.
- [53] H. Mohimani, M. Babaie-Zadeh, and C. Jutten. A fast approach for overcomplete sparse decomposition based on smoothed l0 norm. *IEEE Trans. Signal Process.*, 57(1):289–301, January 2009.
- [54] L. B. Montefusco, D. Lazzaro, and S. Papi. A fast algorithm for nonconvex approaches to sparse recovery problems. *Signal Processing*, 93(9):2636–2647, 2013.
- [55] N. Mourad and J. P. Reilly. Minimizing nonconvex functions for sparse vector reconstruction. *IEEE Trans. Signal Process.*, 58(7):3485–3496, July 2010.
- [56] M. Nikolova. Estimation of binary images by minimizing convex criteria. In *Proc. IEEE Int. Conf. Image Processing (ICIP)*, pages 108–112 vol. 2, 1998.
- [57] M. Nikolova. Markovian reconstruction using a GNC approach. *IEEE Trans. Image Process.*, 8(9):1204–1220, 1999.
- [58] M. Nikolova. Energy minimization methods. In O. Scherzer, editor, *Handbook of Mathematical Methods in Imaging*, chapter 5, pages 138–186. Springer, 2011.
- [59] M. Nikolova, M. K. Ng, and C.-P. Tam. Fast nonconvex nonsmooth minimization methods for image restoration and reconstruction. *IEEE Trans. Image Process.*, 19(12):3073–3088, December 2010.
- [60] X. Ning, I. W. Selesnick, and L. Duval. Chromatogram baseline estimation and denoising using sparsity (BEADS). *Chemometrics and Intelligent Laboratory Systems*, 139:156–167, December 2014.
- [61] D. P. Palomar and Y. C. Eldar, editors. *Convex Optimization in Signal Processing and Communications*. Cambridge University Press, 2010.
- [62] A. Parekh and I. W. Selesnick. Convex denoising using non-convex tight frame regularization. *IEEE Signal Processing Letters*, 22(10):1786–1790, October 2015.
- [63] A. Parekh and I. W. Selesnick. Convex fused lasso denoising with non-convex regularization and its use for pulse detection. <http://arxiv.org/abs/1509.02811>, October 2015.
- [64] J. Portilla and L. Mancera. L0-based sparse approximation: two alternative methods and some applications. In *Proceedings of SPIE*, volume 6701 (Wavelets XII), San Diego, CA, USA, 2007.
- [65] J. Portilla, V. Strela, M. J. Wainwright, and E. P. Simoncelli. Image denoising using scale mixtures of Gaussians in the wavelet domain. *IEEE Trans. Image Process.*, 12(11):1338–1351, November 2003.

- [66] K. Qiu and A. Dogandzic. Sparse signal reconstruction via ECME hard thresholding. *IEEE Trans. Signal Process.*, 60(9):4551–4569, September 2012.
- [67] B. D. Rao, K. Engan, S. F. Cotter, J. Palmer, and K. Kreutz-Delgado. Subset selection in noise based on diversity measure minimization. *IEEE Trans. Signal Process.*, 51(3):760–770, March 2003.
- [68] A. Repetti, M. Q. Pham, L. Duval, E. Chouzenoux, and J.-C. Pesquet. Euclid in a taxicab: Sparse blind deconvolution with smoothed l1/l2 regularization. *IEEE Signal Processing Letters*, 22(5):539–543, May 2015.
- [69] I. W. Selesnick. Sparsity-assisted signal smoothing. In R. Balan et al., editors, *Excursions in Harmonic Analysis, Volume 4*. Birkhäuser Basel, 2015.
- [70] I. W. Selesnick and I. Bayram. Sparse signal estimation by maximally sparse convex optimization. *IEEE Trans. Signal Process.*, 62(5):1078–1092, March 2014.
- [71] I. W. Selesnick, A. Parekh, and I. Bayram. Convex 1-D total variation denoising with non-convex regularization. *IEEE Signal Processing Letters*, 22(2):141–144, February 2015.
- [72] L. Sendur and I. W. Selesnick. Bivariate shrinkage functions for wavelet-based denoising exploiting interscale dependency. *IEEE Trans. Signal Process.*, 50(11):2744–2756, November 2002.
- [73] Y. She. Thresholding-based iterative selection procedures for model selection and shrinkage. *Electronic Journal of Statistics*, 3:384–415, 2009.
- [74] C. Soussen, J. Idier, D. Brie, and J. Duan. From Bernoulli-Gaussian deconvolution to sparse signal restoration. *IEEE Trans. Signal Process.*, 59(10):4572–4584, October 2011.
- [75] X. Tan, W. Roberts, J. Li, and P. Stoica. Sparse learning via iterative minimization with application to MIMO radar imaging. *IEEE Trans. Signal Process.*, 59(3):1088–1101, March 2011.
- [76] J. Trzasko and A. Manduca. Highly undersampled magnetic resonance image reconstruction via homotopic L0-minimization. *IEEE Trans. Medical Imaging*, 28(1):106–121, January 2009.
- [77] S. Voronin and R. Chartrand. A new generalized thresholding algorithm for inverse problems with sparsity constraints. In *Proc. IEEE Int. Conf. Acoust., Speech, Signal Processing (ICASSP)*, pages 1636–1640, May 2013.
- [78] Y. Wang and W. Yin. Sparse signal reconstruction via iterative support detection. *SIAM J. Imag. Sci.*, 3(3):462–491, 2010.
- [79] D. Wipf and S. Nagarajan. Iterative reweighted ℓ_1 and ℓ_2 methods for finding sparse solutions. *IEEE J. Sel. Top. Signal Processing*, 4(2):317–329, April 2010.
- [80] J. Woodworth and R. Chartrand. Compressed sensing recovery via nonconvex shrinkage penalties. <http://arxiv.org/abs/1504.02923>, April 2015.
- [81] H. Zou and R. Li. One-step sparse estimates in nonconcave penalized likelihood models. *Ann. Statist.*, 36(4):1509–1533, 2008.